Beamline 7.0.1

Surface and Materials Science, Spectromicroscopy, Spin Resolution, Photon-Polarization Dichroism

Cu metallic quantum well states on Cu/Ni/Cu(100) and Cu/Fe/Cu(100)
Danese, A., R.A. Bartynski, D.A. Arena, M. Hochstrasser, J. Tobin

Investigation of surface and bulk half-metallic character of Fe_3O_4 by spin resolved photoemission
Morton, S.A., G.D. Waddill, S. Kim, I.K. Schuller, S.A. Chambers, J.G. Tobin

Lateral inhomogeneities and termination in ultrathin block copolymer films
Fink, R., Th. Schmidt, N. Rehse, G. Krausch, I. Koprinarov, H. Ade

Magnetic properties of Fe_3O_4 films grown by epitaxial electrodeposition on the low index planes of gold
Switzer, J.A., T.A. Sorenson, S.A. Morton, G.D. Waddill

Photoelectron Spectroscopy of Plutonium at the Advanced Light Source
Tobin, J.G., D.A. Arena, B. Chung, P. Roussel, J. Terry, R.K. Schulze, J.D. Farr, T. Zocco, K. Heinzelman, E. Rotenberg, D.K. Shuh

Polarization-dependent soft-x-ray absorption of highly oriented ZnO microrod-array
Guo, J.-H., L. Vayssieres, C. Persson, R. Ahuja, B. Johansson, J. Nordgren

Quantum confinement observed in α-Fe_2O_3 nanorod-array
Guo, J.-H., L. Vayssieres, C. Såthe, S.M. Butorin, J. Nordgren.

Soft x-ray emission spectroscopy of ions in solution
Augustsson, A., J.-H. Guo, D. Spandberg, K. Hermansson, J. Nordgren

Spin-resolved electronic structure studies of ultrathin films of Fe on singular and vicinal GaAs
Spangenberg, M., E.A. Seddon, E.M.M. McCash, T. Shen, S.A. Morton, D. Waddill, J. Tobin

Surface spectroscopy of nano-scale reactions in aqueous solution
Pecher, K.H., B. Tonner

Variable moments and changing magnetic behavior of thin-film FeNi alloys
Hochstrasser, M., J.G. Tobin, N.A.R. Gilman, R.F. Willis, S.A. Morton, G.D. Waddill

X-ray magnetic linear dichroism of Fe-Ni alloys on Cu(111)
Johnson, T.F., Y. Sato, S. Chiang, M. Hochstrasser, J.G. Tobin, J.A. Giacomo, J.D. Shine, X.D. Zhu, D.P. Land, D.A. Arena, S.A. Morton, G.D. Waddill

X-ray spectromicroscopy of branched polyolefin blends
Appel, G., I. Koprinarov, G.E. Mitchell, A.P. Smith, H. Ade

Cu Metallic Quantum Well States on Cu/Ni/Cu(100) and Cu/Fe/Cu(100)

A. Danese,[1] R.A. Bartynski,[1] D.A. Arena,[2] M. Hochstrasser,[2] and J. Tobin[2]
[1] Department of Physics and Laboratory for Surface Modification
Rutgers University, 136 Frelinghuysen Rd., Piscataway, NJ 08855
[2]Lawrence Livermore National Laboratory

Ultrathin metal films grown epitaxially on metal substrates often exhibit so called metallic quantum well (MQW) states.[1-8] These are electronic states that are confined to the overlayer by reflectivity from projected band gaps in the substrate metal. Even in the absence of such band gaps, significant interface reflectivity can from intense quantum well resonances. Owing to band structure effects, a given MQW state will move to higher energy as the thickness of the overlayer increases. Furthermore, the periodicity with which these states cross the Fermi level is expected to be a function of the overlayer band structure and insensitive to the substrate.

Much of the work on MQW states has concentrated on the behavior of Cu on various transition metal substrates such as Ni and Co, owing to their importance in magnetic multilayers. In the unoccupied electronic states above the Fermi level, the Cu/Ni(100) system is unusual in that the Cu-induced levels disperse downward with increasing film thickness, rather than downward.[9, 10] It was thought that this might be due to strain in the Cu film. To test these ideas, we used photoemission and inverse photoemission to study the occupied and unoccupied overlayer electronic states of the Cu/Ni/Cu(100) system as a function of Cu and Ni thickness.

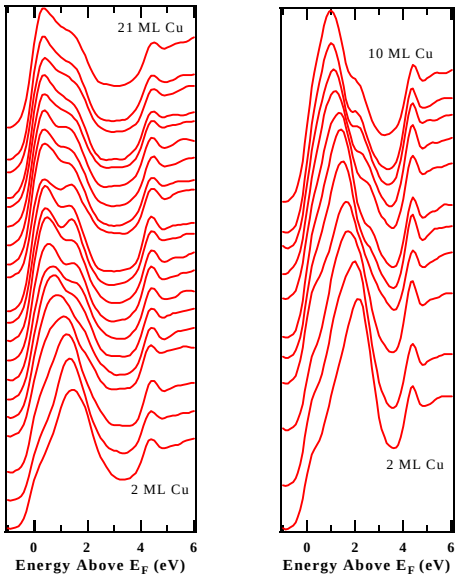

Fig. 1: Downward dispersion of unoccupied Cu states in the Cu/Ni/Cu(100) system.

In Fig. 1 we show inverse photoemission spectra from increasingly thick Cu overlayers on a 35 ML and on a 5 ML film of Ni grown on Cu(100). One can see that the results are qualitatively similar to eachother, and to the Cu/Ni(100) results, in that the Cu-induced states disperse downward as a function of increasing Cu film thickness. There are quantitative differences, however. The states of the Cu films grown on the thinner Ni layer are at higher energy than those on the thicker Ni film. Although it appears that the downward dispersion does not appear to arise from a strain effect, these quantitative differences may. To test this, we measured normal emission photoemission from wedges of Cu grown on two different thickness Ni films on the same Cu(100) substrate. A diagram of the sample geometry is shown in Fig. 2. Two identical Cu wedges were grown on Ni films of 7 ML and 35 ML thicknesses.

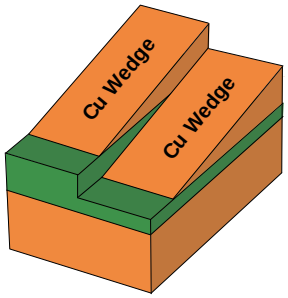

FIG.2: Sample geometry for photoemission studies.

Using the UltraESCA end station of Beamline 7.0.1, we have obtained photoemission data from the Cu/fccNi/Cu(100) system. The sample was prepared by depositing the Ni onto an atomically

clean, well-ordered Cu(100) surface. This was followed by deposition of a wedge-shaped Cu film whose thickness ranged from 0 to 40+ ML. Figure 3 show a series of normal emission photoemission data displayed as a 2-dimensional plot of Cu film thickness vs. binding energy. Light colors indicate high intensity and the dark colors low. These peaks are associated with metallic quantum well states in the Cu films. In contrast to the inverse photoemission data, the intensity maxima that move towards the Fermi level as the film thickness increases. Although the MQW states are less pronounced on the thicker Ni film, the period with which these Cu MQW states cross E_F appears are identical. As a change in the Cu lattice constant would change the electronic structure and thus change the periodicity of the Fermi level crossings, these results suggest that there is minimal change in strain in these Cu films. Strain in the Ni, however, may cause this effect. Quantitative structural studies and first principles electronic structure calculations are currently underway to investigate the low energy structures of these systems.

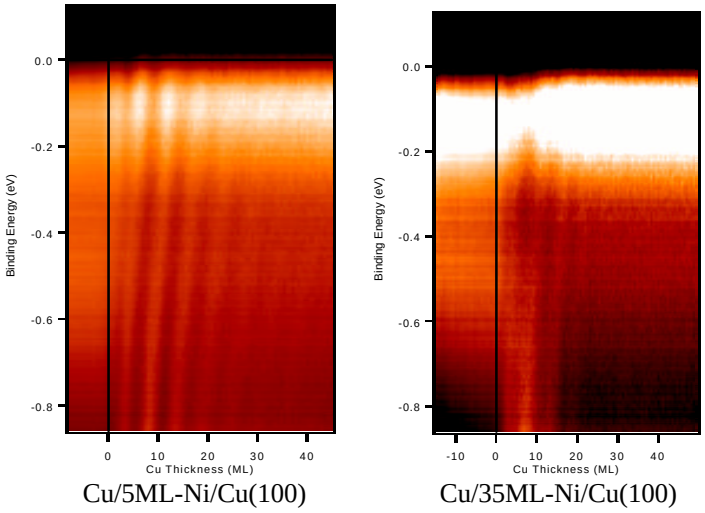

Fig. 3.: Normal emission from the Cu/Ni/Cu(100) systems as a function of Cu film thickness.

Another important observation is the sharp contrast between the upward dispersion of Cu MQW states below the Fermi level and the downward dispersion of Cu state above E_F. Most likely this difference arises because the Ni *d*-bands terminate about E_F + 0.1 eV. The downward dispersion if the Cu states on Ni is most likely associated with the interaction of the Cu and Ni *sp*-band.

Finally, we have also grown Cu/fccFe/Cu(100) quantum well structures and the exhibit a strong upward dispersion and cross EF with a periodicity that is, within experimental uncertainty, the same as that of the Cu/Ni system.

REFERENCES

[1] J.E. Ortega and F.J. Himpsel, Phys. Rev. Lett. **69**, 844 (1992).
[2] P. Segovia, E.G. Michel and J.E. Ortega, Phys. Rev. Lett. **77**, 2734 (1996).
[3] F.G. Curti, A. Danese and R.A. Bartynski, Phys. Rev. Lett. **80**, 2213 (1998).
[4] R.K. Kawakami et al., Phys. Rev. Lett. **80**, 1754 (1998).
[5] R.K. Kawakami et al., Nature. **398**, 132 (1999)
[6] R.K. Kawakami et al., Phys. Rev. Lett. **82**, 4098 (1999).
[7] A. Danese and R.A. Bartynski, Phys. Rev. B. (in press).
[8] A. Danese, D.A. Arena and R.A. Bartynski, Prog. Surf. Sci. **67**, 249 (2001).
[9] O. Rader and F.J. Himpsel, Appl. Phys. Lett. **67**, 1151 (1995).
[10] C. Hwang and F.J. Himpsel, Phys. Rev. B **52**, 15368 (1995).

This work is supported by NSF Grant DMR-98-01681 and Petroleum Research Fund Grant # 33750-AC5,6.

Principle Investigator: Robert A. Bartynski, Department of Physics and Laboratory for Surface Modification, Rutgers University. Email: bart@physics.rutgers.edu. Telephone: 732-445-4839

Investigation of Surface and Bulk Half-metallic Character of Fe_3O_4 by Spin Resolved Photoemission

S. A. Morton (a), G. D. Waddill (a), S. Kim (b), Ivan K. Schuller (b), S. A. Chambers (c) and J. G. Tobin (d)

(a) Department of Physics, U. of Missouri-Rolla, Rolla, MO 65409, USA
(b) Department of Physics, U. of California San Diego, La Jolla, CA 92093, USA
(c) Pacific Northwest National Laboratory, Richland, WA 99392, USA
(d) Lawrence Livermore National Laboratory, Livermore, CA 94550 USA

The existence of a new class of magnetic materials displaying metallic character for one electron spin population and insulating character for the other was first postulated by DeGroot *et al* [1] in 1983 based on theoretical band structure calculations of the ferromagnetic Heusler alloy NiMnSb. Since then such half metallic materials, which by definition posses 100% electron polarization at the Fermi energy have attracted considerable theoretical, experimental, and technological interest as potential pure spin sources for use in spintronic devices [2], data storage applications, and magnetic sensors. In addition to Heusler alloys half metallic character has also been predicted to occur in a wide range of manganites [3], metallic oxides [4], and CMR systems [5]. However, such predictions have proven to be extremely difficult to confirm experimentally [6]. A major factor in this failure has proven to be significant experimental challenges in obtaining a clean stoichiometric surface with a magnetization that is truly representative of the bulk material and thus suitable for further study by magneto-optical or spectroscopic techniques.

In recent experiments at the ALS we have used spin resolved photoemission to study the role that surface reconstruction plays in the observed polarization of the half metallic candidate material magnetite, Fe_3O_4. Magnetite has a structure that is relatively simple in comparison to most other candidate half metals and it can be grown epitaxially using conventional deposition techniques [7], making it one of the strongest candidates for spintronic applications. However previous spin resolved measurements have shown that the polarization at the Fermi edge is only ~40% [8] rather than the anticipated 100%.

By conducting spin resolved depth profile measurements and comparing the results to theoretical band structure calculations we have demonstrated that Fe_3O_4 exhibits a semiconducting non-magnetic surface re-construction which significantly reduces the observed polarization but that, in contrast, the underlying bulk material is in fact very strongly polarized. Indeed, once the effects of this surface reconstruction are taken into account by theoretical models of the polarization an excellent match is obtained between the experimental spin resolved spectra and simulated spectra generated from theoretical spin polarized band structure calculations [9] (fig. 1). Hence our results strongly support the notion that Fe_3O_4 is indeed a half-metallic material suitable for use in a new generation of spintronic devices.

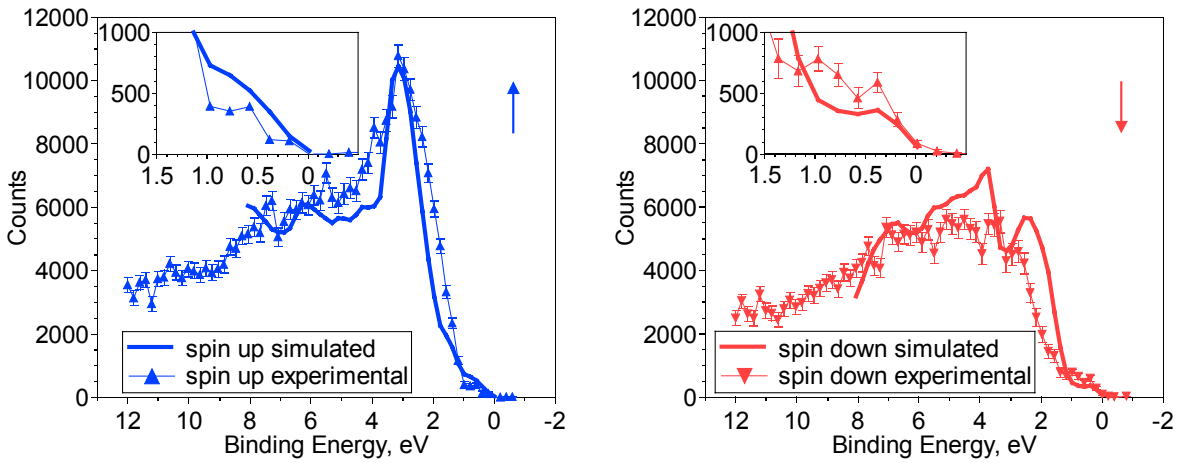

Figure 1

Comparison of experimental spin resolved Fe_3O_4 valence bands with equivalent simulated spectra derived from theoretical calculations that have been corrected to account for the presences of a nonmagnetic surface reconstruction

References

1. R. A. de Groot *et al., Phys. Rev. Lett*. **50,** 2024 (1983).
2. S. A. Wolf, D. Treger, *IEEE Trans. Mag*. **36** 2748 (2000).
3. S. Jin *et al*., *Science* **264,** 413 (1994).
4. Z Zhang, S. Satpathy, *Phys. Rev. B* **44**, 13319 (1991).
5. W. E. Pickett, D. J. Singh, *Phys. Rev. B* **53**, 1146 (1996).
6. K. P. Kamper *et al.*, *Phys. Rev. Lett.* **59** 2788 (1987).
7. S. A. Chambers, S. A. Joyce, *Surf. Sci.* **420,** 111 (1999).
8. S. F. Alvarado *et al*., *Phys. Rev. Lett*. **34,** 319 (1975).
9. S.A. Morton *et al*., *Submitted to Surface Science Letters*

This work was supported by the Director, Office of Energy Research, Office of Basic Energy Sciences, Materials Science Division, of the U.S. Department of Energy under Contract No. # R5-32633.A02. This work was performed under the auspices of the U.S Department of Energy by Lawrence Livermore National Laboratory under contract no. W-7405-Eng-48.

Principal Investigator: Ivan K. Schuller, Department of Physics, University of California San Diego, La Jolla, CA 92093. Phone: (858) 534-2540 fax: (858) 534-0173 Email: ischuller@ucsd.edu

Lateral inhomogeneities and termination in ultrathin block copolymer films

R. Fink[1], Th. Schmidt[1], N. Rehse[2], G. Krausch[2], I. Koprinarov[3], H. Ade[4]

[1]Experimentelle Physik II, Universität Würzburg, Am Hubland, D-97074 Würzburg, Germany
[2]Physikalische Chemie II, Universität Bayreuth, D-95440 Bayreuth, Germany
[3]Brockhouse Institute for Materials Research, McMaster Univ., Hamilton, ON L8S 4M1, Canada
[4]North Carolina State Univ., Dept. Of Physics, Raleigh, NC 27695 , USA

INTRODUCTION

Linear chain-like molecules consisting of blocks of chemically different components (so-called block-copolymers) in many cases form long-range ordered supramolecular structures. The reason for this behavior is the interplay between phase separation of the different components and the molecular unity in the single molecules. The size of the forming structures depends on the size of the molecules and ranges from about 10 to 100 nm. This is usually called "microphase separation" or "micro domain formation". Due to the differences in the surface free energy of the polymers the structure of the micro domains of the surfaces and interfaces can be manipulated. Whereas the structure and morphology of diblock copolymers has been intensely investigated, the investigation of more complex structures (multiblock copolymers, graft polymers, star-like copolymers, etc.) has started only recently.

Recent investigations demonstrate more complex surface and thin film morphologies [1-3]. E.g., an ABC-triblock copolymer consisting of polystyrene (PS), polybutadiene (PB) and polymethylmethacrylate (PMMA), which forms lamellar-like structures in bulk, forms lateral structures at the surface, since the PB-center block (PB) has the lowest surface free energy [4]. To investigate these structures, microscopic techniques with none or only limited spectral sensitivity have been employed so far (atomic force microscopy, scanning electron microscopy, transmission electron microscopy). Although these techniques offer a limited potential to distinguish the polymer blocks, a definite and unambiguous attribution of the respective polymer subunits is still lacking.

EXPERIMENTS

We have used the unprecedented opportunities of high brilliance synchrotron radiation at the Advanced Light Source in particular the installed microspectroscopes (PEEM2 at BL 7.3.1.1 and STXM at BL 7.0.1) to investigate the stoichiometric inhomogeneities in those films within the bulk (STXM) and in the surface-near region (PEEM). Our preliminary experiments have explicitely demonstrated the usefulness of these microspectroscopic techniques.

Fig. 1 shows a STXM image of a thin film consisting of a PS-PB-PMMA triblock copolymer (floated on a 100 nm thick Si_3N_4 membrane) recorded at a photon energy of 293 eV (image size: 60 x 60 μm^2). The lower image shows a cross section along the red bar clearly indicating the distinct film thicknesses in the sample. This finding is in accordance with the lamellar structure which is formed in bulk of those materials. Brighter spots give a clear indication of an additional lateral fine structure within the homogenous areas. The structures in the upper left corner of Fig. 1 are due to partial dewetting of single terraces.

Fig. 2 shows two XPEEM images recorded at the positive and negative slope of the prominent π^*-resonance ($h\nu$ = 286.5 eV) reflecting a distinct contrast reversal which ist due to the different termination of the various terraces, i.e. in one case the terrace consists mainly of the PS species whereas in the other areas PMMA is the prominent species. Images recorded at the O K-edge

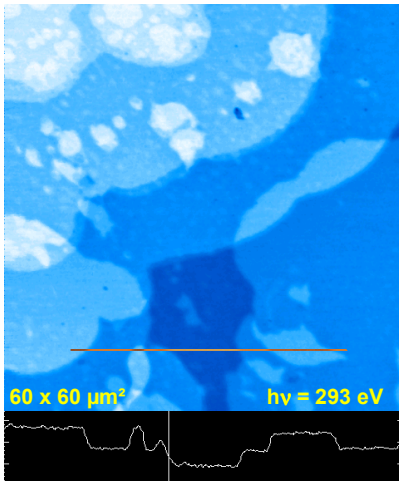

Fig.1: STXM image of a PS-PB-PMMA-triblock copolymerfilm.

allow much higher magnification due to the higher photon flux and thus allow direct imaging of the lateral patterning, which is dominated by the dewetting of the organic film. The finding of differently terminated areas is fully consistent with previous indirect conclusions drawn from AFM data and thus represents a direct spectroscopic proof.

In both cases, PEEM and STXM, the microdomain formation within a terrace with periodicities on the order of up to several 10 nm can at present not be resolved. XPEEM of soft matter films at present is limited to lateral resolutions of about 100 nm and, in addition, may lead to misinterpretations of the spectroscopic data since the high photon flux densities lead to fast degradation/fragmentation of the organic molecules or even conversion into graphite. STXM partly overcomes the latter restriction since the illumination time is significantly shorter. Much higher transmission (by a factor 100 to 1000 at comparable magnification) of the electron optics in an aberration-corrected XPEEM (like, e.g., at PEEM3 or SMART) will improve spectroscopic imaging of surfaces of soft matter films.

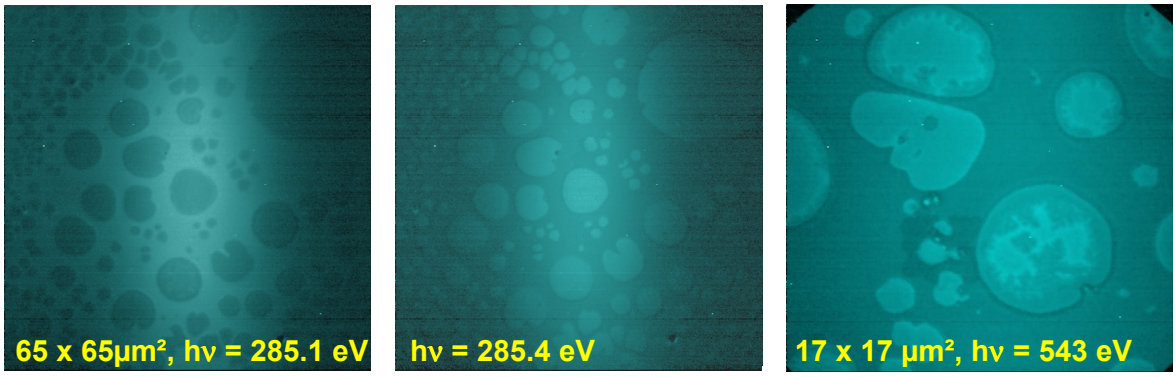

Fig. 2: PEEM images of a PS-PB-PMMA triblock copolymer film indicating the spectroscopic contrast (contrast reversal in the XPEEM images by 0.3 eV photon energy variation). Left and center: excitation at the C K-edge; right:excitation at the O K-edge at higher magnification.Note, that the surface has been plasma-etched to remove the top PB layer.

REFERENCES

[1] W. Stocker, J. Beckmann, R. Stadler, J.P. Rabe, *Macromolecules* **29,** 7502 (1996).

[2] H. Elbs, K. Fukunaga, G, Sauer, R. Stadler, R. Magerle, G. Krausch, *Macromolecules* **32,** 1204 (1999).

[3] K. Fukunaga, H. Elbs, G. Krausch; *Langmuir* **16,** 3474 (2000).

[4] N. Rehse, A. Knoll, R. Magerle, G. Krausch; *Phys. Rev. Lett.* **87.** 035505 (2001)

This work was supported by the Bundesminister für Bildung und Forschung, contracts 05SL8WW18 and 05KS1WCA1. We gratefully acknowledge experimental support by A. Scholl and A. Doran during the experiments at PEEM2. Many thanks to A.P. Hitchcock for providing the AXIS 2000 program for data evaluation.

Principal investigator: Rainer Fink. Experimentelle Physik II, Universität Würzburg.
Email: raifi@physik.uni-wuerzburg.de Telephone: +49-931-888-5163.

Magnetic Properties of Fe_3O_4 Films Grown by Epitaxial Electrodeposition on the Low Index Planes of Gold

J.A. Switzer[1], T.A. Sorenson[1], S.A. Morton[2], and G.D. Waddill[2]
[1]Department of Chemistry and Graduate Center for Materials Research
[2]Department of Physics and Graduate Center for Materials Research
University of Missouri-Rolla, Rolla, Missouri 65409-1170, USA

Spin-dependent charge transport is currently receiving a lot of attention due to potential applications in giant magnetoresistive (GMR) devices such as magnetic field sensors, magnetoresistive random access memories (MRAM), read heads, and galvanic isolators.[1,2] These devices require a source of spin-polarized electrons. Magnetite, Fe_3O_4, is a promising source of spin-polarized carriers, because density-functional theory spin-resolved density of states calculations have suggested that electrons at the Fermi level are -100% spin polarized.[3,4] Magnetite is a mixed-valence 3d transition metal oxide that has an inverse spinel structure (space group *Fd3m*) with a lattice constant of 0.8397 nm. The tetrahedral sites of the spinel structure are entirely occupied by Fe^{3+}, whereas the octahedral sites are occupied half by Fe^{2+} and half by Fe^{3+}. Fe_3O_4 undergoes a metal-to-insulator Verwey transition at 120 K and the Curie temperature of magnetite is 860 K. Recently, GMR effects greater than 500% have been reported at room temperature for Fe_3O_4 nanocontacts.[5]

We have electrodeposited galvanostatically epitaxial Fe_3O_4 films on Au(111), a system with a 3% lattice mismatch.[6] These films are ~0.5 μm thick and have a (111) orientation. X-ray diffraction and SEM results establish that the magnetite films consist of twinned domains rotated by 180° with respect to each other. For the spin-polarized photoemission measurements a magnetic field from an *in situ* electromagnet is applied to the sample either in the plane of the sample or perpendicular to that plane. The field is then removed and the photoemission measurements are performed in remanence. The spin-resolved measurements were done at Beamline 7.0.1 with the spin-resolved endstation.[7] The energy of the excitation beam was ~ 160 eV. Emitted photoelectrons were collected and filtered by a PHI 10-360 SCA hemispherical electron energy analyzer and then passed into a micro-Mott detector to resolve the electron spins. The total energy resolution for the spin resolved measurements was ~0.5 eV. Finally we have measured Fe L edge and O K edge XAS as well as Fe MXCD for these samples at Beamline 4.0. For the MXCD measurements, the sample was magnetized *in situ* and the measurements were made in remanance. All measurements were made at room temperature. Prior to the photoemission, XAS, and MXCD measurements the samples are briefly sputtered and then annealed in an oxygen environment. This produces LEED patterns consistent with the presence of rotationally twinned Fe_3O_4(111), but the films are rather poorly ordered. Photoemission always observes a trace amount of surface carbon.

The Fe L edge and O K edge XAS are shown in Figs. 1 and 2 respectively. In Fig. 3 we show the Fe L edge MXCD. These results are virtually indistinguishable from results reported by Kim *et al*. for a bulk magnetite sample.[8] Figs. 4 and 5 show the spin-resolved photoemission results for these samples. The polarization at the Fermi level is approximately – 40% with a change in the sign of the polarization observed at ~1 eV binding energy. The reasons for the observed deviation from the predicted value of –100% is not known. There are two recent repots for *in situ* prepared Fe_3O_4 films that report either – 50%[9] or – 80%[10] spin-polarization. The first result

is attributed to correlation effects that set an upper limit on the spin-polarization of – 67%[11] while the latter is regarded as evidence for half-metallic behavior. The discrepancy between these various results requires further investigation.

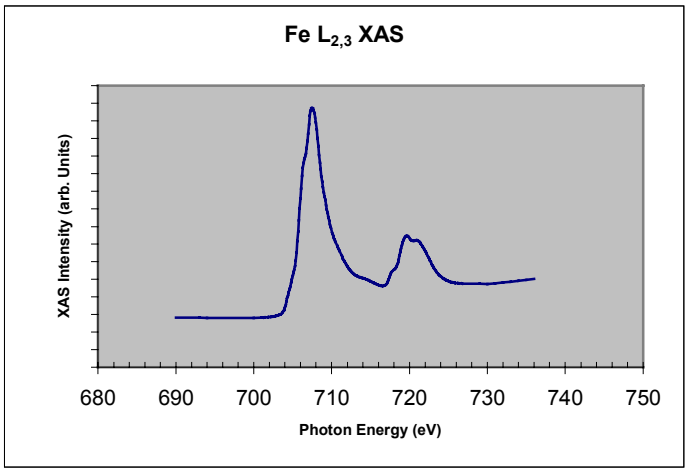

Figure 1. Fe L edge x-ray absorption for thick magnetite film on Au(111).

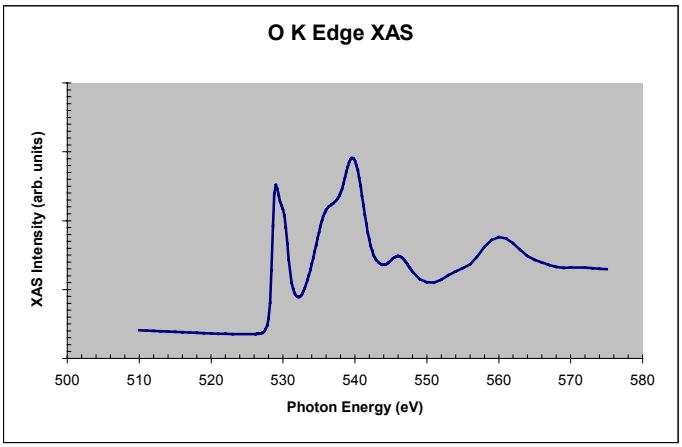

Figure 2. O K edge x-ray absorption for thick magnetite film on Au(111).

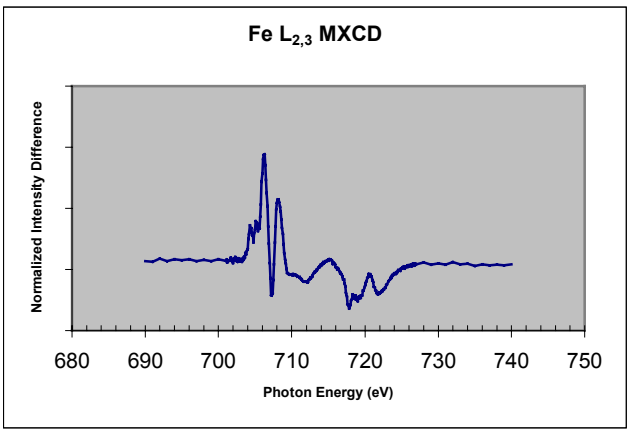

Figure 3. Fe L edge magnetic x-ray circular dichroism for thick magnetite film on Au(111).

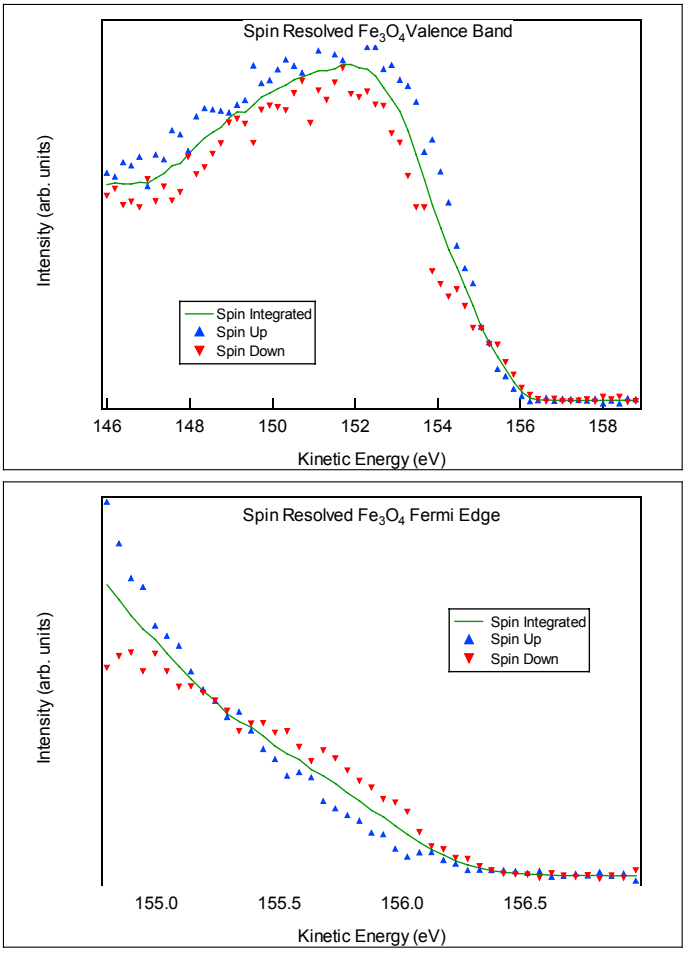

Figure 4. Spin-resolved valence band and Fermi edge for magnetite on Au(111).

REFERENCES

1. G.A. Prinz, Science **282**, 1660 (1998).
2. S.A. Wolf, D.D. Awschalom, R.A. Buhrman, J.M. Daughton, S. von Molnar, M.L. Roukes, A.Y. Chtchelkanova, D.M. Treger, Science **294**, 1488 (2001).
3. Z. Zhang and S. Satpathy, Phys. Rev. B **44**, 13319 (1991).
4. V.I. Anisimov, I.S. Elfimov, N. Hamada, and K. Terakura, Phys. Rev. B **54**, 4387 (1996).
5. J.J. Versluijs, M.A. Bari, and J.M.D. Coey, Phys. Rev. Lett. **87**, 026601 (2001).
6. M.P. Nikiforov, A. Vertegel, M.G. Shumsky, and J.A. Switzer, Adv. Mater. **12**, 1351 (2000).
7. J.G. Tobin, P.J. Bedrossian, T.R. Cummings, G.D. Waddill, S. Mishra, P. Larson, R. Negri, E. Peterson, P. Boyd, and R. Gunion, MRS Symp. Proc. **524**, 185 (1998).
8. H.J. Kim et al., Phys. Rev. B61, 15284 (2000).
9. D.J. Huang, L.H. Tjeng, J. Chen, C.F. Chang, W.P. Wu, A.D. rata, T. Hibma, S.C. Chung, S.-G. Shyu, C.-C. Wu, and C.T. Chen, Surf. Rev. Lett. (in press).
10. Y.S. Dedkov, U. Rudiger, and G. Guntherodt, Phys. Rev. B **65**, 064417 (2002).
11. S.F Alvarado, W. Eib, F. Meier, D.T. Pierce, K. Sattler, H.C. Siegmann, J.P. Remeika, Phys. Rev. Lett. **34**, 319 (1975).

The National Science Foundation (CHE 9816484, DMR 0071365, and DMR 0076338) and the Foundation for Chemical Research are gratefully acknowledged for financial support of this work.

Principal investigator: Dan Waddill, Department of Physics and Graduate Center for Materials Research, University of Missouri-Rolla. Telephone: 573-341-4797. Email: waddill@umr.edu.

Photoelectron Spectroscopy of Plutonium at the Advanced Light Source

J.G. Tobin[*,1], D.A. Arena[1,#], B.Chung[1], P. Roussel[1,&], J. Terry[2,+], R.K. Schulze[2], J. D. Farr[2], T. Zocco[2], K. Heinzelman[3], E. Rotenberg[3], D.K. Shuh[3]

[1]*Lawrence Livermore National Laboratory, Livermore CA, USA*
[2]*Los Alamos National Laboratory, Los Alamos NM, USA*
[3]*Lawrence Berkeley National Laboratory, Berkeley, CA, USA*

We are developing a program to perform Photoelectron Spectroscopy and X-Ray Absorption Spectroscopy upon highly radioactive samples, particularly Plutonium, at the Advanced Light Source in Berkeley, CA, USA. First results from alpha and delta Plutonium are reported as well as plans for a dedicated spectrometer for actinide studies.

I. Introduction

Photoelectron Spectroscopy and X-Ray Absorption are being used to investigate the electronic structure of alpha and delta Pu. [It is generally believed that alpha is more free electron like and delta is possibly a correlated electronic system, although this has yet to be unequivocably proven and the details of which remain clouded.] Our preliminary results[1], where Resonant Photoemission was used to probe large grain polycrystalline delta and polycrystalline alpha, have lead us to modify our initial plans. For example, during the last year we have embarked upon a building project, developing a dedicated Pu Spectrometer at the Advanced Light Source. One result of our first studies is that we believe that minimization of sample oxidation is a key to successful experimentation and we are pursuing that vigorously. Additionally, it now appears that a new experiment, based upon "Double Polarization," may be the key to differentiating between the several models now being proposed to explain the electronic structures of alpha and delta Pu. Here the combination of a chiral xray environment and true spin detection will allow us to test whether spin-orbit, exchange, coulombic repulsion or other multielectronic effects drive the differences between alpha and delta Pu.

II. Experimental

The first experiments were performed at the Spectromicroscopy Facility (Beamline 7.0) at the Advanced Light Source in Berkeley, CA[2]. The Pu samples were taken from a specially purified batch of Pu metal. The plutonium was zone refined and vacuum distilled while magnetically levitated[3] . The product of the purification process was α-Pu containing a total of 170 ppm impurities. A portion of the refined metal was alloyed with gallium to form the δ-phase (fcc symmetry). The sample surfaces were prepared by repeated room-temperature, sputter-annealing cycles to minimize the amount of oxygen and other impurities dissolved in the sample or at grain boundaries, in a specially designed chamber attached to the sample introduction and analysis systems on Beamline 7.0. The transfer, preparation, and analysis chambers ensured that the Pu metal samples did not experience pressures greater than 10^{-8} torr. This minimized any surface contaminants that could adversely effect the soft x-ray measurements.

III. Discussion

Using the tunabilty of synchrotron radiation, it is possible to perform many variants of photoelectron spectroscopy and x-ray absorption, including accessing the core levels of the sample constituents. One of the variants that was pursued was Resonant Photoemission.[4] Photoelectron spectroscopy is a "photon in, electron out" process. Often, it can be simplified down to a single electron phenomenon, where the energy of the photon is absorbed and transferred over entirely to a single electron, while all other "spectator" electrons essentially remain frozen. An advantage of this is its simplicity of interpretation. But in many systems, it is possible to induce a process with heightened sensitivity and significantly increased cross sections: resonant photoemission (ResPes)[4-8] . Here, a second set of indirect channels open up, which contribute in concert with the original or direct channel of simple photoemission. Shown in Figure 1 is a schematic illustrating the resonant photoemission process in Pu, involving the 5f and 5d electrons.

The Pu5f5f5d resonant photoemission process occurs over the photon energy range of 90eV to 150eV, with an antiresonance near 100eV and a resonace maximum near 120eV. (See Figure 2.) In our experiments, both alpha and delta Pu samples have been investigated. The valence band ResPes Spectra (Figure 3) exhibit only small differences between the alpha and delta phase samples. These observations correlate well with the recent results of Gouder et al[9], Arko et al[10] and earlier work of L.E. Cox[11], which suggest that surface reconstruction may be an important issue in Pu samples. Nevertheless, subtle yet possibly significant differences can be observed between the α and single crystallite δ samples, particularly at the Fermi energy and near a photon energy of 130eV. These results suggest that the valence electronic structure of Pu is dependent upon its phase and chemical state. Overall the two sets of spectra strongly resemble each other and confirm the observation of Pu 5f ResPes.

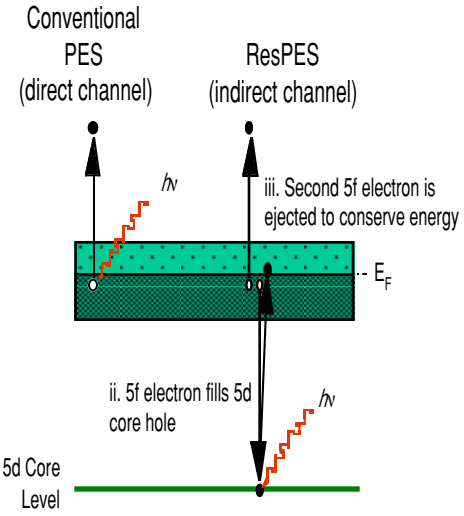

Figure 1. The Resonant Photoemission (ResPes) process for the Pu 5f and 5d states is shown here.

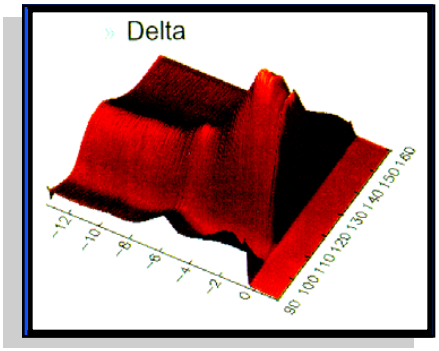

Figure 2. Resonant Photoemission or ResPes is a type of spectroscopic interrogation of the valence electronic structure. A large data set is shown here, for single crystallite delta. The plots show the intensity variations (z axis) versus the binding energy of the states (the negative numbers in eV; zero is the Fermi energy) and photon energy(between 90eV and 160eV).

The similarity of the alpha and delta samples raises an unsettling question. Are the phase actually what we think they are? A means to address this issue and related surface quality questions is to investigate the core level spectroscopy of the Pu and possible additional elemental constituents. Some our results are shown in Figure 4 below.

The spectra in Figure 4a confirm that we have phase specific samples. The alpha and delta are each consistent with earlier reported results[12-15]. Furthermore, the wide scan (Fig 4b) and details of the O1s (Fig 4c) and C1s (Fig 4d) regions at 1250eV confirm that our samples are quite "clean." However, the spectra at 850eV illustrate an interesting point: by tuning to energies where the O1s and C1s cross sections are larger, there is a significant improvement in sensitivity to oxygen and carbon surface degradation. In the future, this will permit us to study surface oxide and carbide formation with improved and lower detection limits.

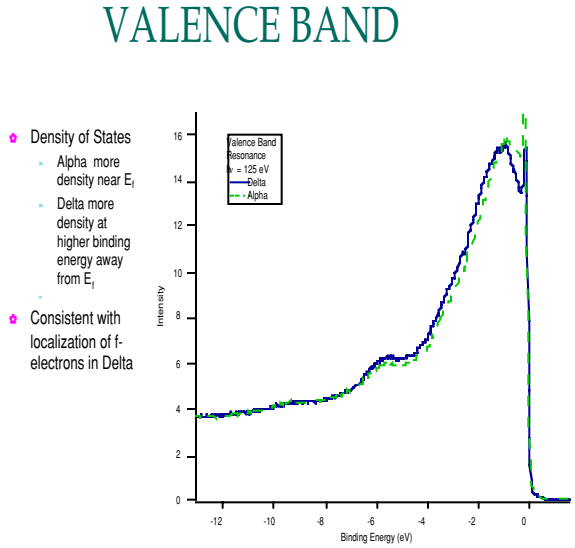

Figure 3. Comparison of the valence band spectra of alpha and delta Pu at a photon energy of 125eV.

Finally, we are presently constructing a new dedicated Pu Spectrometer, a schematic of which is shown in Figure 5. This spectrometer will include specialized capabilities for handling Pu samples. For example, the long vertical manipulator will allow the isolation of the radioactive byproducts of sample preparation and cleaning from the analysis station yet also permit rapid access of the analysis position, so as to minimize surface corruption after cleaning. The photoelectron detection will include capabilities for both multichannel, spin-integrated analysis as well as true spin resolved spectroscopy using a MiniMott detection scheme[16].

IV. Acknowledgements

This work was performed under the auspices of the U.S Department of Energy by LLNL (Contract No. W-7405-Eng-48), LANL (Contract No. W-7405- ENG-36) and LBNL (Contract No. DE-AC03-76SF00098). The Spectromicroscopy Facility (Beamline 7.0) and the Advanced Light Source were built and and are supported by the DOE Office of Basic Energy Research. The authors wish to thank Jason Lashley and Michael Blau for synthesis of the Pu samples.

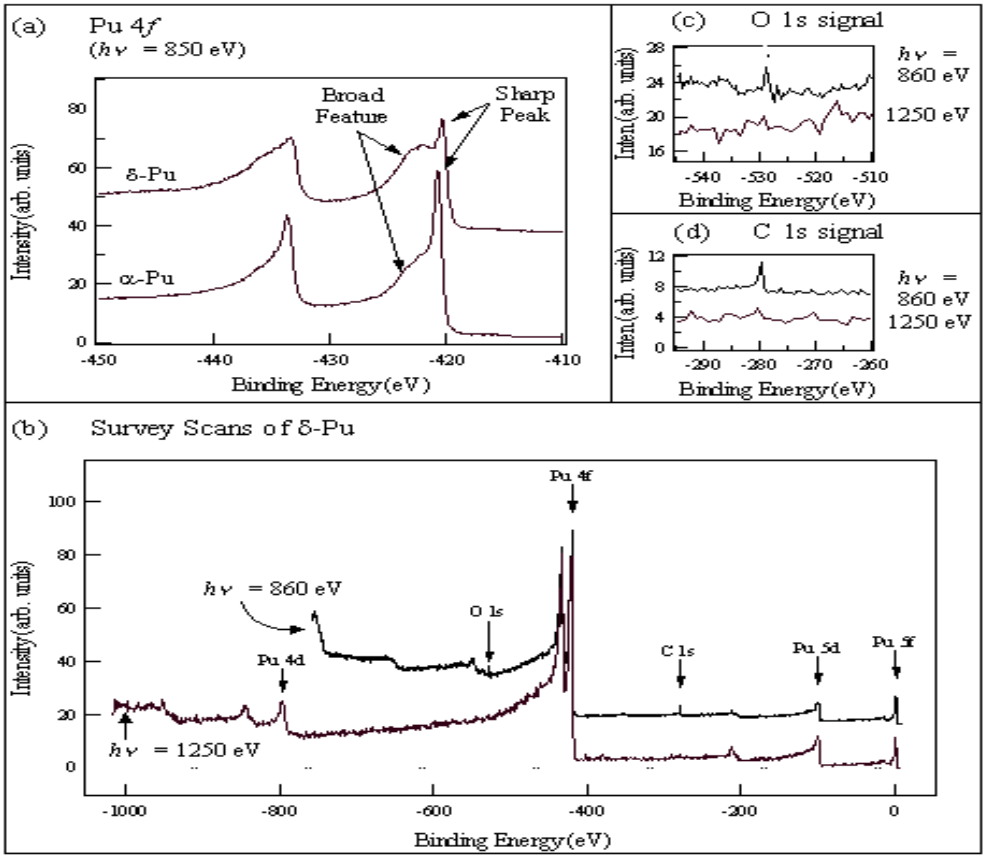

Figure 4 (Left). Core level photoelectron spectroscopy. (a) Detail of the 4f levels of the alpha and delta Pu. (b) Wide scans at both 1250 eV and 860 eV. (c) Detail of the O 1s peak region. (d) Detail of the C 1s peak region.

Figure 5 (Below). Schematic of the new, dedicated Pu Spectrometer.

V. References

- J. Terry, R. K. Schulze, J. D. Farr, T. ZoccoK. Heinzelman, E. Rotenberg, D. K. Shuh, G. Van der Laan,D.A. Arena, and J.G. Tobin, UCRL-JC-140782, submitted to Surface Science Letters, September 2001.
- J.D. Denlinger et al, Rev. Sci. Instrum. **66**, 1342 (1995).
- J.C. Lashley, J. Nucl. Matl. **274**, 315 (1999).
- S.R. Mishra et al., Phys Rev. Lett. **81**, 1306(1998) and references therein.
- G. van der Laan et al.,Phys. Rev. B **46**, 9336 (1992).
- K. Starke et al.,Phys. Rev. B **55**, 2672 (1997).
- G. van der Laan et al. Phys. Rev. B **59**, 8835 (1999); Phys. Rev. B **33**, 4253 (1986).
- A.J. Arko etal.,J. Alloys Cmpds **271-273**, 826 (1998) and **286**, 14 (1999).
- T. Gouder, L. Havela, F. Wastin, and J. Rebizant, Europhys. Lett. 55, 705 (2001).
- A. Arko et al, Phys. Rev. B 62, 1773 (2000).
- L.E. Cox et al, Phys. Rev. B **46**, 13571 (1992).
- T. Gouder et al, J. Alloys Cmpds. **271-273**, 841 (1998); J. El. Spect. Rel. Phen. **101-105**, 419 (2000); Poster Presentation, VUV-12 Conference, San Francisco, CA, 1998.
- R. Baptist et al., J. Phys. F (Metal Phys.) **12**, 2103 (1982).
- L.E. Cox, Phys. Rev. B **37**, 8480 (1988).
- J.R. Naegele, J. Nucl. Matl. **166**, 59 (1989).
- J.G. Tobin and F.O. Schumann, Surf. Sci. **478**. 211 (2001); J.G. Tobin et al, MRS Symp. Proc. **524**, 185 (1998)

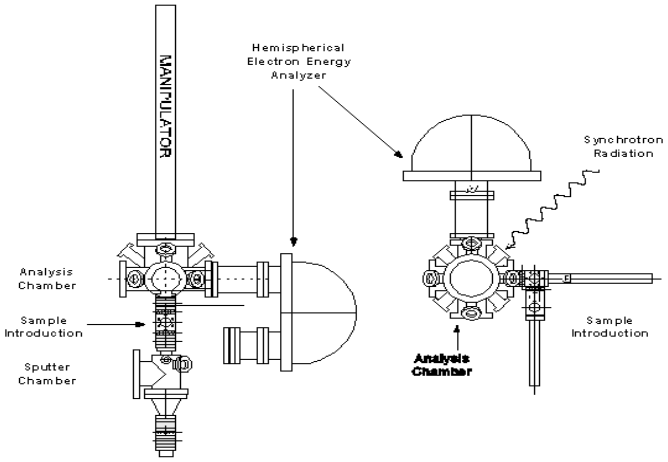

*Corresponding Author: LLNL, L-357, POB 808, 7000 East Ave., Livermore, CA, USA; Tobin1@LLNL.Gov.
[#]Present Address: NRL, Washington, DC, USA
[&]Permanent Address: Atomic Weapons Establishment, United Kingdom
[+]Present Address: IIT, Chicago, IL, USA

Polarization-dependent soft-x-ray absorption of highly oriented ZnO microrod-array

J.-H. Guo[1], L. Vayssieres[2], C. Persson[2], R. Ahuja[2], B. Johansson[2], and J. Nordgren[2]
[1]Advanced Light Source, Lawrence Berkeley National Laboratory, Berkeley, CA 94720
[2]Department of Physics, Uppsala University, Box 530, S-75121 Uppsala, Sweden

Zinc oxide represents an important basic material (II-VI semiconductor) due to its low cost, wide bandgap as well as its electrical, optoelectronic and luminescent properties. ZnO is of importance for fundamental research as well as relevant for various fields of industrial and high technological applications. Recently, a low threshold lasing action has been observed at room temperature in highly oriented ZnO nanorod arrays. From a fundamental point of view, it is crucial to probe and understand the electronic structure of such novel materials to tailor their physical properties as well as developing novel and improved devices. A novel approach to materials chemistry has been developed which contributed to the fabrication of purpose-built nano/microparticulate thin films from aqueous solution[1]. Such well-defined and well-ordered materials should contribute to reach required enhanced fundamental knowledge of the relation between structure and physical properties.

Here we report a polarization-dependent x-ray absorption spectroscopy (XAS) study performed at synchrotron radiation facility on highly oriented ZnO microrods. The experiments were performed on BL7.0.1 at the ALS[2]. The x-ray absorption spectra were measured by recording the total electron yield while scanning the photon energy over the O *1s*-edge region at a resolution of 0.2 eV. The XAS experiments were carried out on two different (isotropic and anisotropic) homogeneous and crystalline zincite ZnO (wurtzite) thin film samples, i.e. ZnO spheres, which consist of monodisperse spherical particles of 150 nm in diameter, and ZnO microrods consisting of monodisperse, anisotropic and highly oriented crystallites grown along the c-axis and perpendicular to a transparent conducting glass substrate (F-SnO2)\cite{Vayssieres01a}. The microrods of 10 μm in length and 1.5 μm in width are oriented normal to the substrate surface.

The polarization-dependent x-ray absorption measurements are shown in Figure 1. The variations in the spectral shape continue up to 30 eV above the absorption threshold. The resolved absorption features are indicated as a_1-a_8. Prior to a_1, no polarization-dependence is observed in x-ray absorption spectra for either sample. However at higher photon energies, strong anisotropic effects are observed for the ZnO microrods (bottom spectra). Measuring at grazing incidence geometry, i.e. incidence angle $\theta = 10$ degrees, where the absorption features a_3, a_5, and a_8 are stronger, the excitation to the state along the *c*-axis of the wurtzite structure is enhanced. At normal incidence geometry, i.e. $\theta = 90$ degrees, where the absorption features a_2, a_4, and a_7 are stronger, the excitation to the in-plane state is enhanced. No significant change is observed for the isotropic samples of ZnO consisting of spherical particles as a function of the polarization angle. However, all the absorption features are averaged out and observed in the

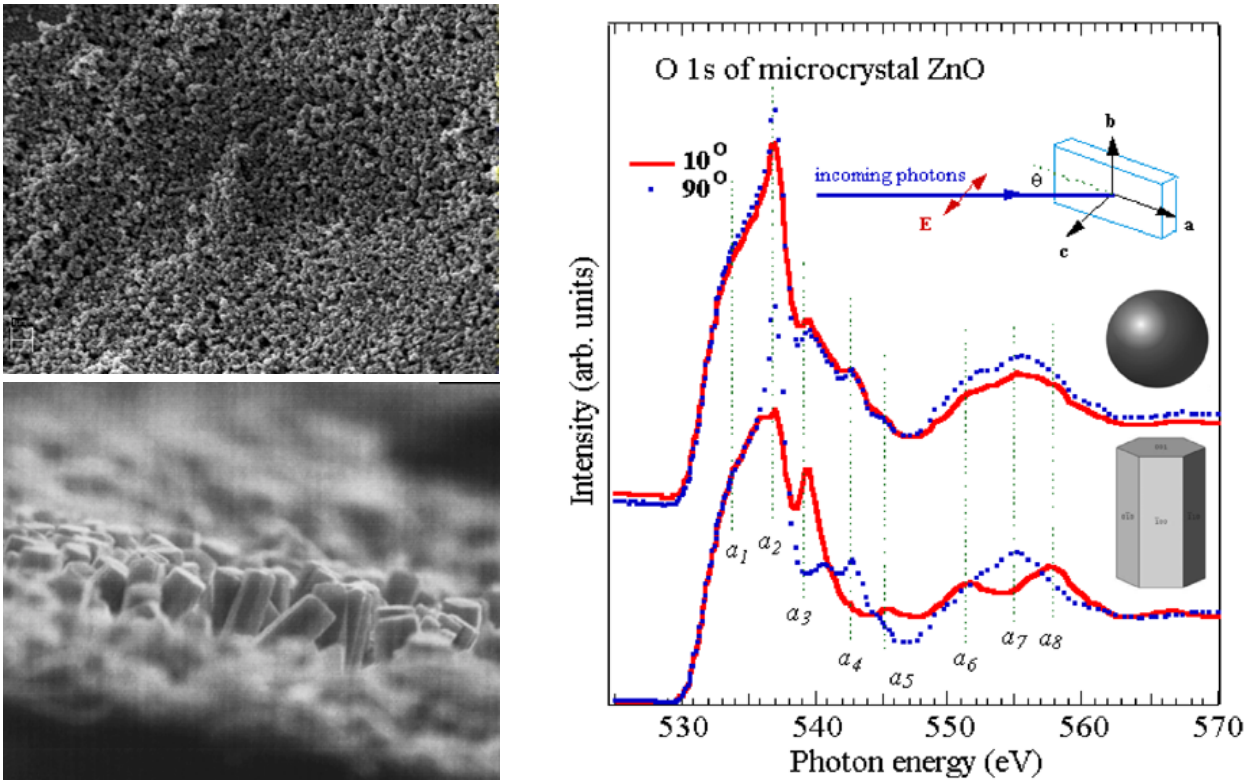

Fig. 1. Polarization-dependent x-ray absorption measurements.

XAS spectra measured with either geometrical detection. The experimental findings suggest a strong correlation between the electronic structure and the geometrical structure of the crystalline ZnO arrays. Such results demonstrate that designing materials with the appropriate morphology and orientation, i.*e purpose-built* materials, enables to reach better fundamental understanding of nano/microscale materials and their physical properties. Probing the orbital symmetry of oxygen and resolving its contribution to the conduction band of this important large band-gap II-VI semiconductor is of crucial importance for the understanding of its optoelectronic properties.

References:

1. L. Vayssieres, A. Hagfeldt and S. E. Lindquist, Pure Appl. Chem. **72**, 47 (2000).
2. T. Warwick, P. Heimann, D. Mossessian, W. McKinney and H. Padmore, Rev. Sci. Instrum. **66**, 2037 (1995).

This work was supported by the Swedish Natural Science Research Council (NFR), Council for Engineering Sciences (TFR), and the Göran Gustafsson Foundation for Research in Natural Science and Medicine (GGS). Department of Energy Materials Sciences Division Contract DE-AC03-76SF00098.

Principal investigator: Jinghua Guo, Advanced Light Source, LBNL. E-mail: jguo@lbl.gov.
Telephone: 510-495-2230.

Quantum confinement observed in α-Fe_2O_3 nanorod-array

J.-H. Guo[1], L. Vayssieres[2], C. Såthe[2], S. M. Butorin[2], and J. Nordgren[2]
[1]Advanced Light Source, Lawrence Berkeley National Laboratory, Berkeley, CA 94720
[2]Department of Physics, Uppsala University, Box 530, S-75121 Uppsala, Sweden

Resonant inelastic x-ray scattering (RIXS) has been applied to the studies of *dd* excitations in MnO and $SrCuO_2Cl_2$ [1,2]. The lowest-lying electronic excitations can be studied most directly by charge neutral spectroscopies, such as electron energy-loss spectroscopy (EELS) and optical absorption. The dd excitations in transition metal compounds are dipole forbidden and therefore very faint in optical spectroscopy.

α-Fe_2O_3 is an antiferromagnetic charge transfer insulator with a bandgap of 2.1 eV. Hematite crystallises in the trigonal system, rhombohedral R-3c group. The crystal structure is the corundum type (Al_2O_3) and can be described as a hexagonal close packed layering of oxygen with 6-fold co-ordinated iron ions yielding to face and edge-sharing octahedra. In an octahedral symmetry, a d^5-configuration is found to have well-separated dd-excitations. Optical absorption spectroscopy of α-Fe_2O_3 has revealed many transitions ranging from infrared to ultraviolet.

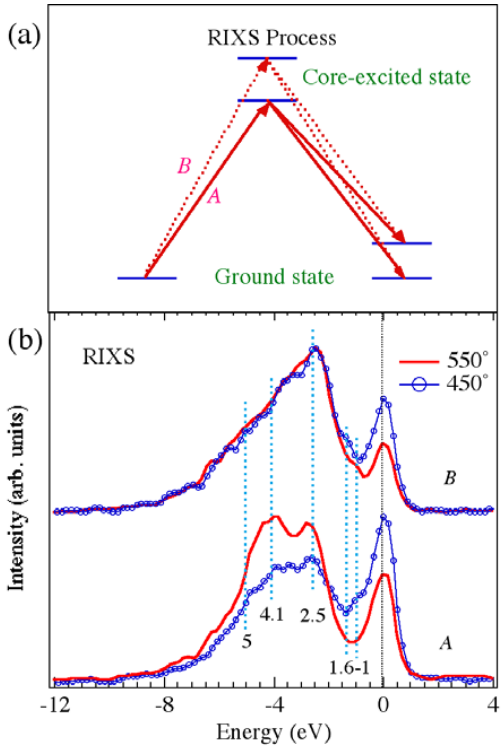

Using the RIXS process, we probed specifically the *dd* excitations in α-Fe_2O_3 by transition sequence $2p^63d^5 \rightarrow 2p^53d^6 \rightarrow 2p^63d^5$. These *dd* transitions become fully allowed, and their intensity can be more easily calculated than that in optical spectroscopy and EELS.

The experiments were performed at beamline 7.0.1 [5] at Advanced Light Source, Lawrence Berkeley National Laboratory. The photon energy resolution was set to 0.2 eV for x-ray absorption spectroscopy (XAS) measurement. The resonant x-ray Raman scattering was measured using a grazing-incidence grating spectrometer [6]. The resolution of both monochromator and fluorescence spectrometer in RIXS measurement was set to 0.5 eV.

The measurements were done on synthetic α-Fe_2O_3 nanorods grown by Controlled Aqueous Chemical Growth [7]. The samples investigated in this letter are thin films, which consist of 3D crystalline array of hematite nanorods bundles of 50 nm in diameter and 500 nm in length perpendicularly oriented onto the substrate. Each bundle was found to consist of self-assembled nanorod of 3-5 nm in diameter. The samples were prepared by

heteronucleation growth and thermodynamic stabilization of akaganeite (β-FeOOH) in solution at 90˚C onto the substrate and subsequently heated in air to 550˚C to allow the crystal phase transition to hematite (α-Fe_2O_3) as confirmed by XRD.

In the resonant inelastic x-ray scattering process, final states probed via such a channel, which are related to eigenvalues of the ground state Hamiltonian. The core-hole lifetime is not a limit on the resolution in this spectroscopy [2]. According to the many-body picture, an energy of a photon, scattered on a certain low-energy excitation, should change by the same amount as a change in an excitation energy of the incident beam (see the decay route of core-excitation *B* versus that of *A* in Fig. 1a). Thus, the RIXS features have constant energy losses and follow the elastic peak.

The RIXS spectra at the Fe *L*-edge of α-Fe_2O_3 nanorods were recorded and shown in Fig.1. A few energy-loss features are clearly resolved. The low energy excitations, such as the strong dd and charge-transfer excitations, are identified in the region from 1 to 5 eV. The 1-eV and 1.6-eV energy-loss features originate from multiple excitation transitions. The 2.5-eV excitation corresponds to the bandgap transition, which is significantly larger than the 2.1-eV-bandgap of single-crystal hematite.

References:

1. S. M. Butorin, J.-H. Guo, M. Magnuson, P. Kuiper, and J. Nordgren, Phys. Rev. B **54**, 4405 (1996).
2. P. Kuiper, J.-H. Guo, C. Såthe, L.-C. Duda, J. Nordgren, J. J. M. Pothuizen, F. M. F. de Groot, and G. A. Sawatzky, Phys. Rev. Lett. **80**, 5204 (1998).
3. L. A. Marusak, R. Messier, and W. B. White, J. Phys. Chem. Solids **41**, 981 (1980).
4. L.-C. Duda, J. Nordgren, G. Dräger, S. Bocharov, Th. Kirchner, J. Electr. Spectros. and Related Phenom. **110-111**, 275 (2000).
5. T. Warwick, P. Heimann, D. Mossessian, W. McKinney and H. Padmore, Rev. Sci. Instrum. **66**, 2037 (1995).
6. J. Nordgren, G. Bray, S. Cramm, R. Nyholm, J. E. Rubensson, and N. Wassdahl, Rev. Sci. Instr. **60**, 1690 (1989).
7. L. Vayssieres, H. Beermann, S.-E. Lindquist, and A. Hagfeldt, Chem. Mater. (in press, 2000).

This work was supported by the Swedish Natural Science Research Council (NFR), Council for Engineering Sciences (TFR), and the Göran Gustafsson Foundation for Research in Natural Science and Medicine (GGS). Department of Energy Materials Sciences Division Contract DE-AC03-76SF00098.

Principal investigator: Jinghua Guo, Advanced Light Source, LBNL. E-mail: jguo@lbl.gov. Telephone: 510-495-2230.

Soft x-ray emission spectroscopy of ions in solution

A. Augustsson[1], J.-H. Guo[1,3], D. Spandberg[2],
K. Hermansson[2] and J. Nordgren[1]

[1]Department of Physics, Uppsala University, Box 530, S-75121 Uppsala, Sweden
[2]Department of Materials Chemistry, Uppsala University, P.O. Box 538, S-75121, Uppsala, Sweden
[3]Advanced Light Source, Ernest Orlando Lawrence Berkeley National Laboratory, University of California, Berkeley, California 94720, USA

INTRODUCTION

Metal-ion transport in both aqueous- and polymer-solvent media involves continuos solvent-ligand exchange. Metal-ion coordination chemistry is therefore fundamental to these phenomena. The application of soft-x-ray absorption spectroscopy (SXAS) and soft-x-ray emission spectroscopy (SXES) to study wet samples has been hampered by the experimental difficulties of handling wet samples under high-vacuum conditions. Optical, infrared and Raman spectroscopies as well as magnetic resonance based methods are often used to determine the structure and the properties of these systems [1]. Here, we report the soft x-ray absorption and emission study of cations (Li^+, Na^+, K^+, Mg^{2+}, and Al^{3+}) in water solution.

Experiment

The experiments were performed at beamline 7.0.1 at the Advanced Light Source (ALS), Lawrence Berkeley National Laboratory. The beamline comprises a 99-pole, 5 cm period undulator and a spherical-grating monochromator [2]. In the liquid phase measurements, the incident photon beam and secondary emission penetrated a thin silicon nitride window of 100 nm in thickness. XAS spectra of liquid water were recorded in x-ray fluorescence yield. XES spectra were recorded using a high resolution grating spectrometer [3].

Cation-solvent interaction

The solvated cation interaction can be monitored by examining the spectra of the solvent. The advantage of this approach is that the restriction to cations no longer applies. For example, it can be used in studying what happens when salts of the alkali and alkaline earth metals are added to aqueous solvent. Series of spectra at different salts at a given concentration exhibit an isosbestic point. In the figure experimental data

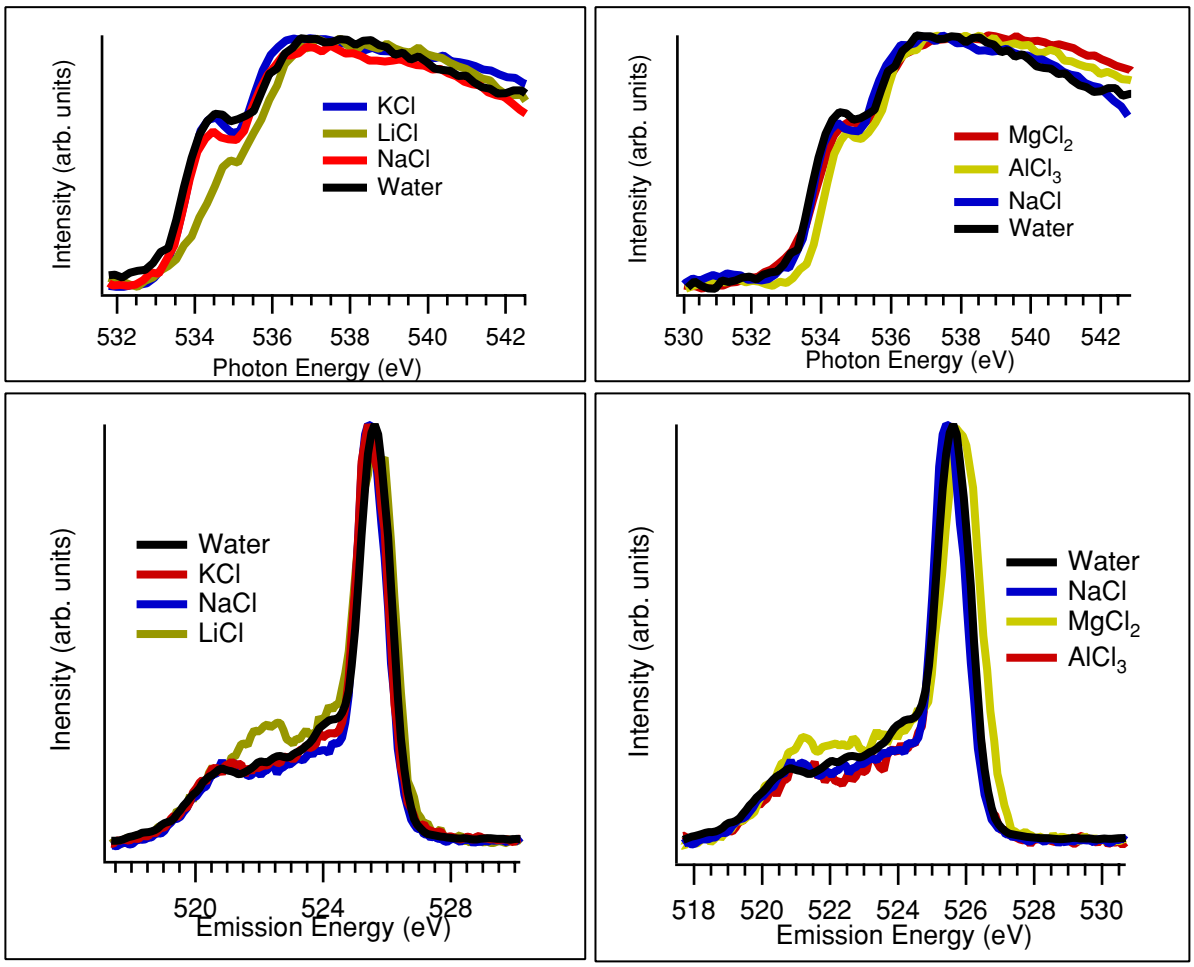

Figure 1: Top panels, O 1s XAS spectrum and bottom panels resonant O K-emission spectra of Ion solutions exited at the photon energy 534.5 eV

from ion-solutions are presented. Spectrum of pure water is also presented for comparison. The bottom panels shows the resonantly excited x-ray emission spectra, excited on the pre-edge in the absorption spectra at $\sim$ 534.5 eV (top panels). The left panel shows a comparison of O 1s spectra of solutions with ions of varying sizes and the right panel shows spectra varying charge. In the emission spectra one observe that spectrum of Na^+ and Al^{3+} solutions are similar while the emission spectrum of the Mg^{2+} solution show a broadened main peak, and some distinct differences at lower energies. Comparing Na^+ and K^+ solutions a small difference is observed, while the smaller Li ion shows a large spectral effect both in absorption and emission. We are presently working with theoretical interpretation, to achieve a full understanding of the data.

References

[1] Jean-Joseph Max and Camille Chapados, J. of Chem. Phys., 115, (2001), p. 2664

[2] T. Warwick and P. Heimann and D. Mossessian and W. McKinney and H. Padmore, Rev. Sci. Instrum. , 66, (1995), p.2037

[3] J. Nordgren and G. Bray and S. Cramm and R. Nyholm and J. -E. Rubensson and N. Wassdahl, Rev. Sci Instum. , 60, (1989), p.1690

This work was supported by the Swedish Research Council (VR), the Göran Gustafsson Foundation for Natural Science and Medicine, and the Swedish Institute.

Principal investigator: E. Joseph Nordgren, Department of physics, Uppsala University, Email: joseph@fysik.uu.se. Telephone: +46 18 4713554.

Spin-resolved electronic structure studies of ultrathin films of Fe on singular and vicinal GaAs

M. Spangenberg[1], E.A. Seddon[1], E.M.M. McCash[2], T. Shen[3],
S.A. Morton[4], D. Waddill[5] and J. Tobin[4]

[1]CLRC Daresbury Laboratory, Keckwick Lane, Daresbury, Cheshire, UK
[2]Department of Chemistry, University of York, Heslington, York, UK
[3]Joule Physics Laboratory, University of Salford, Salford, Greater Manchester, UK
[4]Lawrence Livermore National Laboratory, 7000 East Ave., Livermore, CA 94550
[5]Department of Physics, University of Missouri-Rolla, Rolla, MO 65409

Recently, there has been considerable interest in the study of spin injection at ferromagnetic semiconductor heterojunctions and ferromagnetic metal – semiconductor contacts[1,2,3,4]. Studies of n-type semiconductors have demonstrated spin-coherent transport over large distances[5] and the persistence of spin coherence over a sizeable time scale[6]. Clearly such investigations have been stimulated by the potential of the development of 'spintronics', electronic devices utilising the information of the electron spin states. To understand and improve the magnetic properties of ultrathin Fe films on GaAs has been the aim of many research groups over recent years. The interest in this system has both technological and fundamental scientific motivations. Technologically, Fe on GaAs may serve to realize spin electronic devices. From a fundamental science point of view, Fe on GaAs serves as a prototype for studies of the interplay between the crystalline structure and morphology of an ultrathin film, its electronic structure and the long range magnetic order it exhibits.

In contrast to the attention given to Fe on variously prepared GaAs substrates, the magnetism of Fe on vicinal GaAs substrates has received scant attention. This in spite of the fact that films grown on vicinal substrates present a number of advantages and opportunities. For example, they are known to exhibit enhanced structural homogeneity, surface diffusion tends to follow well mapped patterns (the quasi-periodicity has been exploited to produce quantum wires) and there is an additional degree of control of the film growth beyond those associated with temperature and substrate surface composition[7].

In a preliminary combined spin-polarized secondary electron spectroscopy, photoelectron spectroscopy and LEED study (carried out on the SRS, Daresbury Laboratory) of the remanent magnetic properties of Fe on singular and vicinal (3° offset) GaAs we have shown both that the various magnetic phases formed are dependant upon the Ga to As surface composition of the substrate and that they evolve in characteristic (but not well understood) ways with Fe overlayer thickness[8]. A remarkable feature in this system, which illustrates the importance of the Fe overlayer/substrate interaction, is the magnetic anisotropy; the easy axis of the Fe films on Ga-terminated substrates is perpendicular to that for As-terminated substrates[9,10].

These measurements were followed up with combined spin-resolved photoemission and magnetic linear dichroism experiments on Fe deposited on vicinal (offcut by 3º and 6º) or singular GaAs substrates on Beamline 7 at the ALS in collaboration with Elaine Seddon of CCLRC Daresbury Laboratory, Dan Waddill of The University of Missouri-Rolla and James Tobin Of Lawrence Livermore National Laboratory. The GaAs(100) substrates were available for film deposition at room temperature after substrate decapping *in-situ* (by thermal annealing),

at the ALS. By mounting both singular and vicinal GaAs substrates on the same sample tile the same growth conditions applied for both films facilitating direct comparison. The surface quality was monitored using LEED. The following data were obtained, high resolution spin-integrated valence bands, the spin-resolved valence bands and their energy dispersion, the film thickness dependence of the spin-resolved valence bands, magnetic linear dichroism data on the Fe3p and Fe2p core levels at a variety of photon energies.

The experiments, which were performed with Dr. Simon Morton and Dr. Jim Tobin in November of 2000 have produced considerable amount of interesting results. The significant differences in the spin-resolved valence bands between *ca.*20 Å thick Fe films on singular and vicinal (3º) GaAs are illustrated in Fig.1. As the terrace width is *ca.*55 Å the spectral differences are not due to step-localized features.

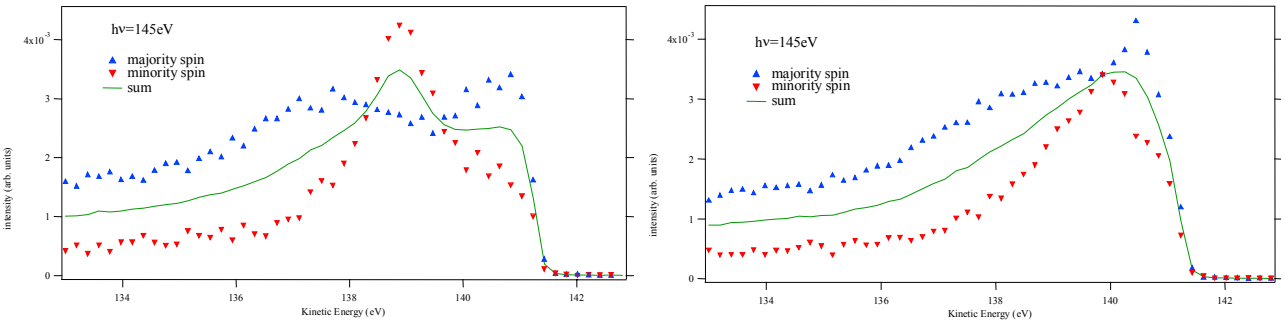

Figure 1
Spin-resolved valence band photoemission results for Fe on singular GaAs (left) and Fe on vicinal (3º) GaAs (right).

Other interesting results include the following. At low film thicknesses, Fe deposited on singular substrates was found to have a lower Curie temperature than Fe on vicinal substrates. Fe deposited on singular substrates reveals a larger energy dispersion of the spin-resolved valence bands than Fe on vicinal substrates. Only marginal differences can be seen between the spin-resolved valence bands of Fe deposited on 3º stepped GaAs substrates and Fe deposited on 6º stepped GaAs substrates. Also, in contrast to the valence band studies, the linear magnetic dichroism results obtained for these samples are very similar.

Further experiments at ALS during oct 2001 enabled us to obtain considerably more interesting results. Whilst the detailed analysis of the results is still underway, Fig.2 shows a large contrast of the valence band spectra of Fe versus incident photon energy between that on a singular and a vicinal substrate. The strong feature on the left in Fig.2 was found to be sensitive to the thickness of the Fe layer and the origin of which is still not yet clear at the present stage.

In summary, the experiments at the ALS have been extremely rewarding. They have answered some questions, clarified our thinking on others and raised yet other questions for which we have no answers at the moment. The run has, however, shown that further access to the ALS is needed to fully understand this fundamental and technologically important system.

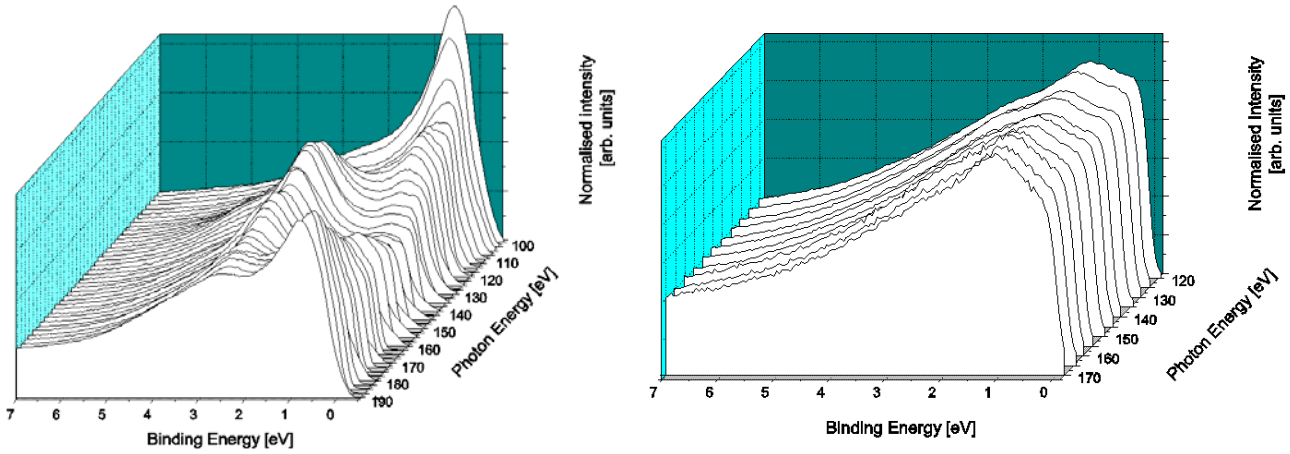

Figure 2.
Valence band spectra of Fe, normalised to the secondary electron tails, versus photon energy for films on singular substrate (left) and on 6 degree vicinal substrate (right).

References:

[1] Malajovich I., Berry J.J., Samarth N. and Awschalom D.D., Nature 411, 770 (2001)
[2] Ohno Y., Young D.K., Beschoten B., Matsukura F., Ohno H. and Awschalom D.D., Nature 402, 790 (1999)
[3] Filip A.T., Hoving B.H., Jedema F.J., van Wees B.J., Dutta B. and Borghs S., Phys. Rev. B 62, 9996 (2000)
[4] Hammar P.R., Bennett B.R., Yang M.Y. and Johnson M., Phys. Rev. Lett. 83, 203 (1999)
[5] Kikkawa J.M. and Awschalom D.D., Nature 397, 139 (1999)
[6] Kikkawa J.M. and Awschalom D.D., Phys. Rev. Lett. 80, 4313 (1998)
[7] Joyce B. A., Neave J. H., Zhang J., Vvedensky D. D., Clarke S., Hugill K.J., Shithara T. and Myers-Beaghton A.K., Semicond. Sci. Technol., **5** 1147 (1990). Kawamura T., Maruta J. and Ishii A., J. Appl. Phys., **39** (7B) 4376 (2000). Gaines J.M., Petroff P.M., Kroemer H., Simes R.J., Geels R.S. and English J.H., J. Vac. Sci. Technol., **B6** 1373 (1998).
[8] Zhang T., Spangenberg M., Greig D., Takahashi N., Shen T-H., Matthew J.A.D., Cornelius S. M., Rendall M. and Seddon, E.A., Appl. Phys. Letters, **78** 961 (2001)
[9] Kneedler E. M., Jonker B. T., Thibado P. M., Wagner R. J., Shanabrook B. V., and Whitman L., J. Phys. Rev. B, **56** 8163 (1997).
[10] Gester M., Daboo C., Hicken R. J., Gray S. J., Ercole A., and Bland J. A. C., J. Appl. Physics **80** 347 (1996).

This work was supported by the Director, Office of Energy Research, Office of Basic Energy Sciences, Materials Science Division, of the U.S. Department of Energy under Contract No. # R5-32633.A02. This work was performed under the auspices of the U.S Department of Energy by Lawrence Livermore National Laboratory under contract no. W-7405-Eng-48. Experiments were carried out at the Spectromicroscopy Facility (Beamline 7.0) at the Advanced Light Source, built and supported by the Office of Basic Energy Science, U.S. Department of Energy.

Principal investigator: E. A. Seddon, CCLRC Daresbury Laboratory, Daresbury, Warrington Cheshire, WA4 4AD, UK, Email: e.a.seddon@dl.ac.uk, Telephone: +44 1925 603245, fax +44 1925 693124

Surface spectroscopy of nano-scale reactions in aqueous solution

K. H. Pecher[1,2] and B. Tonner[2]
[1]currently at: Advanced Light Source, Ernest Orlando Lawrence Berkeley National Laboratory, University of California, Berkeley, California 94720, USA
[2]Depaartment of Physics, University of Central Florida, Orlando, Florida 32816-2385, USA

INTRODUCTION

The rate of oxidation of dissolved Mn(II) by oxygen is enhanced in the presence of catalytic surfaces. Surfaces of iron oxides such as Goethite (α-FeOOH), Lepidocrocite (γ-FeOOH), and Hematite (α-Fe_2O_3) can increase the rate of Mn(II) oxidation over the initial homogeneous solution rate by orders of magnitude [1, 2]. These reactions are further complicated by the observation that initially formed reaction products are metastable and depend strongly on both the bulk reaction conditions such as temperature, concentration of Mn(II), pH-value, presence of dominant anions [3-5], and interfacial reaction conditions existing at the catalytic surfaces. The activities of reactants and products and especially the thermodynamic properties of Mn(III) species at such surfaces are not known and are not readily measurable [4]. In addition, initially formed Mn-oxides or hydroxides may autocatalytically enhance reaction rates [6]. A contribution from autocatalytic oxidation of Mn(II) has been hypothesized for the formation of Mn-micronodules in lake sediments [7] and the occurrence of Mn-biominerals formed by spores of a marine bacillus *SG-1* [e.g. 8, 9]. It is therefore quite natural that details on the identity of reaction products vary a lot in the literature.

Traditionally, two different approaches have been utilized to study Mn(II) oxidation at mineral surfaces: a macroscopic approach using wet chemistry data and surface complexation models [10], and a microscopic approach using Scanning Force Microscopy and surface spectroscopic techniques [11]. Junta-Rosso et al. [12] have also tried to link both microscopic and macroscopic data to develop rate expressions that are consistent with both approaches. The microscopic as well as surface spectroscopic techniques applied in those studies suffer from transfer of wet samples into high vacuum, the effect of which has not yet been studied systematically. We have used Scanning Transmission X-ray Spectromicroscopy (STXM) to characterize products formed during the heterogeneous oxidation of Mn(II) by dissolved oxygen on fully hydrated single nano-sized particles of catalytically active iron oxides.

MATERIALS AND METHODS

Aliquots of powdered iron oxides (Goethite, Lepidocrocite, and Hematite) equivalent to 25 m^2L^{-1} were each suspended in 10 mM HEPES solution (pH 7.8, 50 mM NaCl) and equilibrated for 24 h. Characteristics of the used iron oxides are given elsewhere [13]. These suspensions were kept open to atmosphere on a multi stirring plate and were repeatedly spiked with aliquots from a 55 mM $MnCl_2$ stock solution. Time intervals between sequential addition of Mn(II) were chosen long enough to keep the concentration of dissolved Mn(II) below 0.3 mM.
Two sets of samples were withdrawn for STXM measurements: (a) after 96 d of reaction time and a total Mn(II)-dosage of 244 μM, and (b) after 129 d of reaction time and a total Mn(II)-dosage of 1.26 mM. All X-ray absorption measurements were done at the Advanced Light Source (Lawrence Berkeley National Laboratory) on beam line 7.0.1. Sample preparation and

technical specifications of an upgrade version of STXM are given elsewhere [14, 15]. Data analysis and spectral interpretation using XANES of reference compounds are detailed in [16].

RESULTS AND DISCUSSION

STXM of the first set of samples withdrawn after 96 days and a total Mn(II) dose of 244 μM, did not result in detectable amounts of Mn on the iron oxide particles. Obviously, the mass of adsorbed Mn(II) and/or oxidation products present on the particles were below the detection limit of the instrument. Figure 1 shows single needles of Goethite after 129 d of incubation imaged at the Fe absorption maximum and the corresponding XANES of the Mn-edge. The spectrum could be fitted by a linear combination of spectra of single valent Mn(II) and Mn(III)-reference models. Fits did not improve by including any Mn(IV)-component.

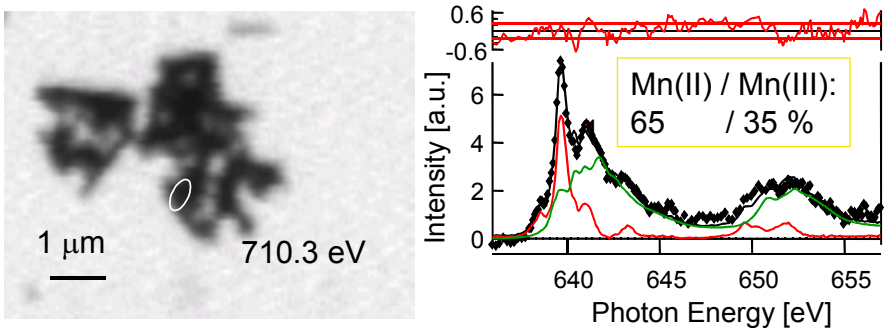

Figure 1. Image of single needles of Goethite (left) and XANES (◆) at the Mn-edge extracted from the area labeled on the image. The XANES is fitted to a linear combination of spectra of single valent reference compounds (red: $MnSO_4$, green: γ-MnOOH). Quantitative results are given in mass % of each charge component and residuals are plotted with the horizontal lines indicating ± one standard deviation.

Under the experimental conditions used, the iron oxide catalyzed oxidation of Mn(II) led to a mixed valent Mn(II)/Mn(III)-species (most likely Hausmannite [4,5]), the stoichiometric ratio of which might be superimposed by specific adsorption of Mn^{2+} from solution. Control experiments under anoxic conditions are necessary to decide whether the high Mn(II)-content is due to adsorption of Mn^{2+} onto iron oxide surfaces or incorporation into oxidation products. Within the time frame of our experiment, we can rule out disproportionation of initial Mn(III)-species, although this reaction is thermodynamically favorable under our bulk reaction conditions. We hypothesize that reaction conditions at the iron oxide interfaces can stabilize Mn(III). Comparing the mass fraction of Mn(III) on all three iron oxides, the order is α-FeOOH»α-Fe_2O_3>γ-FeOOH, which does not correlate with the amount of specific sites for cation sorption on those oxides. The observed order, however, does correlate with the order of catalytic activities observed during reductive dehalogenation of polyhalogenated methanes by Fe(II) sorbed to exactly the same iron oxides [13]. We conclude that unknown steric/electronic properties of the iron oxide substrates might be involved as controlling factors in lowering the redox potential of transition metal cations sorbed to such surfaces.

ACKNOWLEDGMENTS

Thanks to Sirine Fakra, Rick Steele and Tony Warwick for providing such a wonderful instrument. Adam Hitchcock and Eli Rotenberg provided software for data analysis.

REFERENCES

[1] Diem, D.; Stumm, W. Geoch. et Cosmoch. Acta 1984, 48,1571-1573.
[2] Sung, W.; Morgan, J.J. Geoch. et Cosmoch. Acta 1981, 45,2377-2383.
[3] Hem, J.D. Geoch. et Cosmoch. Acta 1981, 45,1369-1374.
[4] Hem, J.D.; Lind, C.J. Geoch. et Cosmoch. Acta 1983, 47, 2037-2046.
[5] Murray, J.W.; Dillard, J.G.; Giovanoli, R.; Moers, H.; Stumm, W. Geoch. et Cosmoch. Acta 1985, 49,463-470.
[6] Murray, J.W. Geoch. et Cosmoch. Acta 1975, 39,505-519.
[7] Murray, L.W.; Balistrieri, L.S.; Paul, B. Geoch. et Cosmoch. Acta 1984, 48,1237-1247.
[8] Nealson, K.H.; Tebo, B.M. Adv. Appl. Microbiol. 1988, 33,279-318.
[9] Mandernack, K.W.; Post, J.; Tebo, B.M. Geoch. et Cosmoch. Acta 1995, 59,4393-4408.
[10] Davies, S.H.R.; Morgan, J.J. J. Colloid Interface Sci. 1989, 129,63-77.
[11] Junta, J.L.; Hochella Jr., M.F. Geochim. Cosmochim. Acta 1994, 58,4985-4999.
[12] Junta-Rosso, J.L.; Hochella Jr., M.F.; Rimstidt, J.D. Geoch. et Cosmoch. Acta 1997, 61,149-159.
[13] Pecher, K.; Haderlein, S. B.; Schwarzenbach, R. P. Environ. Sci. Technol. 2001 accepted.
[14] http://www-esg.lbl.gov/Stxm/
[15] Pecher, K.; Kneedler, E.; Rothe, J.; Meigs, G.; Warwick, T.; Nealson, K.; Tonner, B. In: X-ray Microscopy (XRM´99); AIP Conference Proceedings 507, W. Meyer-Ilse, T. Warwick, D. Attwood (Eds.); Berkeley, 2000; p 291-300.
[16] Pecher, K.; McCubbery, D., Kneedler, E.; Rothe, J.; Bargar, J.; Meigs, G.; Cox, L., Nealson, K.; Tonner, B. submitted to Geoch. et Cosmoch. Acta 2001.

This work was supported by the Director, Office of Energy Research, Office of Basic Energy Sciences, Materials Science Division, of the U.S. Department of Energy under Contract No. DE-AC03-76SF00098. This work was supported by grants from DOE Division of Materials Sciences FG02-98ER45688 and DOE NABIR FG02-97ER62474.

Principal investigator: Klaus Pecher, Advanced Light Source, Ernest Orlando Lawrence Berkeley National Laboratory. Email: khpecher@lbl.gov. Telephone: 510-495-2232.

Variable Moments and Changing Magnetic Behavior of Thin-Film FeNi Alloys

M. Hochstrasser[1], J.G. Tobin[1], N.A.R. Gilman[2], R.F. Willis[2], S.A. Morton[3], and G.D. Waddill[3]
[1]Chemistry & Material Science Division, Lawrence Livermore National Laboratory,
Livermore, California 94550, USA
[2]Department of Physics, The Pennsylvania State University, University Park, Pennsylvania 16802, USA
[3]Department of Physics, University of Missouri-Rolla, Rolla, Missouri 65409, USA

INTRODUCTION

The electronic properties and magnetic behavior of FeNi alloys have been of special interest since 1897 when Guillaume [1] first reported an almost zero thermal expansion over a wide temperature range in face-centered cubic (fcc) crystals with a Ni concentration of around 35 atomic percent. This behavior was subsequently observed in various ordered and random binary alloy systems, and became known as the "Invar Effect" [2]. Despite much experimental [3] and theoretical [4] work, a full understanding of this important technological effect is lacking.

A general view, first advanced by Weiss [3], is that the Fe atoms first develop a large magnetic moment in the Ni-rich alloys, which expands their lattice as their number increases. At a critical Wigner-Seitz cell volume, the strain energy becomes too large and there is a phase transition from this "high-spin/high-volume" state into a 'low-spin/low-volume" state. In the bulk alloys, this instability begins around 60% Fe content, the Curie temperature falling precipitously, simultaneously with a 'martensitic' structural transformation to body-centerd cubic (bcc) symmetry [2]. Theoretical work predicts that the fcc phase can exist in two possible states: a ferromagnetic high volume state or an antiferromagnetic low volume state (2 γ state model) [3] with a volume change between the paramagnetic and the high spin state of ~7% [5], and 1% change between a non-collinear equilibrium state and the high spin state [4]. Experimental work shows a lattice expansion increasing linearly up to 3% at 65% Fe content followed by a sudden relaxation of 2% with increasing Fe content [6]. This work also shows that the martensitic structural transformation can be arrested in ultrathin alloy films epitaxially grown on a Cu(100) substrate. The nanometer-scale thickness effectively 'clamps' the crystal structure to that of the fcc substrate. Small changes in the Wigner-Seitz cell volume produce a small tetragonal distortion, which can be monitored by diffraction methods [6]. By growing ultrathin pseudomorphic fcc films, it is possible to focus on the effect of changing alloy composition on themagnetic and electronic behavior.

Here, we report changes in the magnitudes of both elemental magnetic moments with changing composition, measured with X-ray linear/circular dichroism as well as changes in the exchange splitting measured with spin- and angle-resolved photoemission.

RESULTS AND DISCUSSION

A plot of the change in the asymmetry amplitude, for both elements in the FeNi alloy measured with XMLDAD, being a measure of the expectation value of the atomic magnetic moment $\langle\mu\rangle$, is shown plotted as a function of composition, fig. 1 (left panel). We observe that both the Ni and Fe signals track a similar profile with changing composition. In the Ni-rich alloys, both signal increase linearly up to 65% that on the Fe showing the larger increase. Above 65% Fe content, both signals show a sharp decrease. The observed asymmetry amplitudes, suggest that a high-spin moment develops on the Fe with increasing Fe content that increases overall magnetization,

which then increases the polarization of the valence states surrounding the Ni atomic cores. The Ni thus develops a component that tracks the developing magnetization. Above 65% Fe-content, the high-spin moment on the Fe appears to collapse to a "low-spin value", causing the overall magnetization density to be lowered, which is sensed by the reduced polarization of the valence states on the Ni. A plot of the variation of a 'stoichiometric average moment' $xA(Fe_x)+(1-x)A(Ni_{1-x})$ is shown in fig. 1 (right panel).. The behavior is very similar to that reported for the variation of the saturated moment normalized to the volume of similar fcc films on Cu(100) & Cu(111) and measured with SQUID magnetometry [7]. The solid line is the behavior reported for FeNi alloys from neutron scattering measurements [2]. We note that the Ni-rich phase extrapolates to a value around μ=2.5-3.0μB, a value predicted theoretically for the "high-moment" metastable fcc phase [5]. The above 'mean magnetic moment' variation, normalizing the Ni asymmetry amplitude to be equivalent to the magnetic moment of metallic Ni is tracking closely the Slater-Pauling curve, the moment increasing linearly with increasing number of holes per atom in the valence electronic states. Above 65% Fe content, the average moment shows a sharp decline into a "low-spin" magnitude state, which could be the result of a collapse of the spin moment on the Fe atoms and/or a sudden decrease in magnetization due to a non collinear rearrangement of spins.

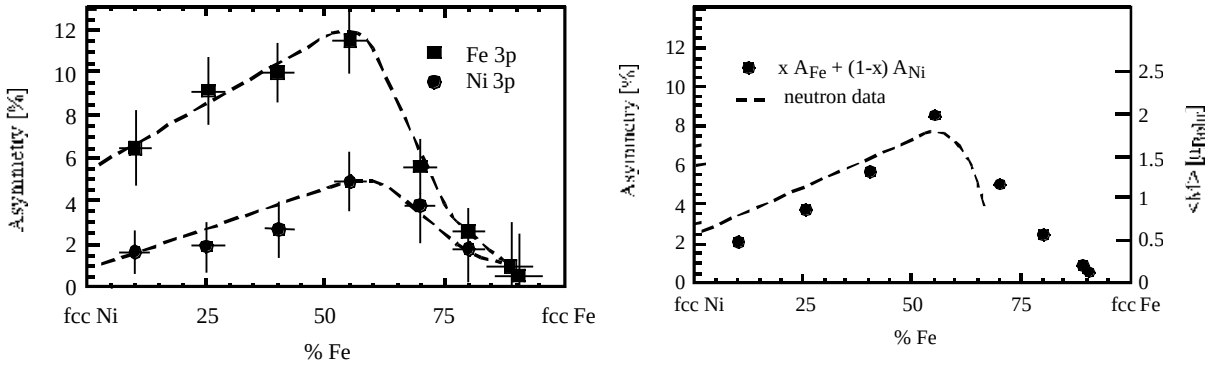

Figure 1. Left panel: Change in dichroism amplitude, A, as a function of FeNi alloy composition. Right panel: The variation of the 'stoichiometrically-weighted' dichroism signal amplitude (see text) with changing FeNi alloy composition. The dashed curve is the behavior observed in bulk FeNi alloys by neutron scattering. The right hand scale is determined from neutron and SQUID magnetometry data [2,7]

Spin polarized photoemission studies record a sudden decrease in the "mean-field" exchange splitting of the d-states with increasing Fe content through the critical "Invar transition". Angle-resolved photoemission imaging of states at the Fermi level [8] reveal a much smaller splitting of the sp-states, which also tracks the changing magnetization with changing composition. Spectral lineshapes reveal a decreased lifetime (i.e. decreased mean-free path for scattering) of the minority spin-polarized sp-states, in agreement with reported similar measurements on permalloy [9].Angle-resolved photoemission measurements of the sp-states, away from the regions of emerging minority d-states, along the <110> (Σ) symmetry direction, resolves the sp exchange splitting in reciprocal space. We observe that the spectral width of the minority-spin band of the sp-states is broader than that of the majority-spin sp-band.

This has been reported in similar measurements on permalloy, and is indicative of a shorter lifetime due to increased scattering and a shorter mean-free-path for the minority spin electrons. We also note that the lifetime broadening of the minority-spin sp-states increases significantly in the Fe rich alloys. The measured exchange splitting of the sp-states as well as the spin-resolved measured exchange splitting of the d-states track the behavior of the x-ray core-level photoemission dichroism.

This is to be expected on the basis of the overall magnetic energy being the sum of a 'local moment' energy on the 'atom(s) and a 'mean-field' exchange energy rising from the spin polarization of the itinerant valence states [10].
X-ray circular dichroism measurements allow to separate the orbital from the spin part of the local moments. Our measurements show the same concentration dependence of the local moments as t he linear dichroism measurements.

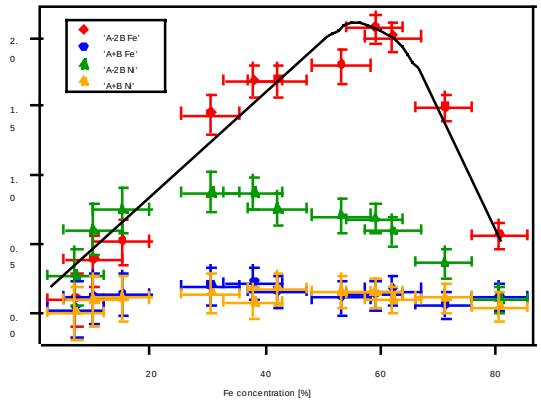

Figure 2. The variations of the spin, respectively orbital parts of the magnetic moments. [A-2B=-C/$\mu_B(\mu_s+\mu_D^{\alpha})$; A+B=-3C/2$\mu_B(\mu_O^{\alpha})$]. A, B are the areas underneath the difference peaks of the 2p spectra taken with magnetization up and down.

REFERENCES

1. C.E. Guillaume, C.R. Acad. Sci. **125**, 235 (1897)
2. E.F. Wassermann in "Ferromagnetic Materials", Vol. 5, K.H. Buchow & E.P. Wohlfarth (eds.), Elsevier, Amsterdam (1990)
3. R.J. Weiss, Proc. R. Soc. London, Sect. A **82**, 281 (1963)
4. M. van Schilfgaarde, I.A. Abrikosov and B. Johansson, Nature 400, 46 (1999)
5. I.A. Abrikosov, O. Erikson, P. Sonderling, H.L, Skriver, & B. Johansson, Phys. Rev. B51,1058 (1995)
6. F.O. Schumann, R.F. Willis, K.G. Goodman, & J.G. Tobin, Phys. Rev. Lett. **79**, 5166 (1997)
7. J.W. Freeland, I.L. Grigorov, & J.C. Walker, Phys. Rev. **B57**, 80 (1998)
8. M. Hochstrasser, N. Gilman, R.F. Willis, F.O. Schumann, J.G. Tobin, & E. Rotenberg, Phys. Rev. **B60**, 17030 (1999)
9. D.Y. Petrovykh, K.N. Altmann, H. Höchst, M. Laubscher, S. Maat, G.J. Mankey, & F.J. Himpsel, Appl. Phys. Lett. **73**, 3459 (1998)
10. "Ferromagnetism" by R.M. Bozorth, Van Nostrand (1951)

This work was supported by the Director, Office of Energy Research, Office of Basic Energy Sciences, Materials Science Division, of the U.S. Department of Energy under Contract No. *# R5-32633.A02*. This work was performed under the auspices of the U.S Department of Energy by Lawrence Livermore National Laboratory under contract no. W-7405-Eng-48. Experiments were carried out at the Spectromicroscopy Facility (Beamline 7.0) and at Beamline 4 at the Advance Light Source, built and supported by the Office of Basic Energy Science, U.S. Department of Energy.

Principal investigator: J.G. Tobin, Chemistry & Material Science Division, Lawrence Livermore National Laboratory, Livermore, California 94550, USA, Email: tobin1@llnl.gov, Telephone: 925 422 7247

X-ray Magnetic Linear Dichroism of Fe-Ni Alloys on Cu(111)

T.F. Johnson,[*] Y. Sato,[*] S. Chiang,[*] M. Hochstrasser, [#] J.G. Tobin[#], J.A. Giacomo,[*]
J.D. Shine,[*] X.D. Zhu,[*] D.P. Land,[**] D.A. Arena,[♦] S.A. Morton,[♣] G.D. Waddill[♣]
*Dept. of Physics, University of California, Davis
**Dept. Of Chemistry, University of California, Davis
#Lawrence Livermore National Laboratory, Livermore
♣University of Missouri, Rolla
♦Brookhaven National Laboratory, Upton, NY

INTRODUCTION

We are studying layer-by-layer synthesis of ultra-thin metal films by controlling at the monolayer level the composition and structure of these films, including the interfacial region. We have prepared Fe_xNi_{1-x} multilayers using simultaneous evaporation of pure Fe and Ni on Cu(111) in order to better understand the Giant Magnetoresistance (GMR) effect in FeNi/Cu systems that are relevant to magnetic disk drive heads. Using Undulator Beamline 7.0 and the Spin Spectroscopy Facility (7.0.1.2) at the ALS, we have measured X-ray Magnetic Linear Dichroism (XMLD) signals for twenty three different thin Fe-Ni alloys films on Cu(111) for different thicknesses and with Fe concentration ranging from 9% to 84%. X-ray Photoelectron Spectroscopy (XPS) with 1250 eV photon energy was utilized to determine both thickness and elemental composition. The Fe3p and Ni3p lines were measured for magnetization up and down, and the difference is the XMLD signal. Our XMLD spectra clearly indicate that samples of specific thicknesses and Fe concentrations are ferromagnetic. XMLD has previously been used to characterize Fe_xNi_{1-x} alloy fcc multilayers on Cu(100)[1].

RESULTS

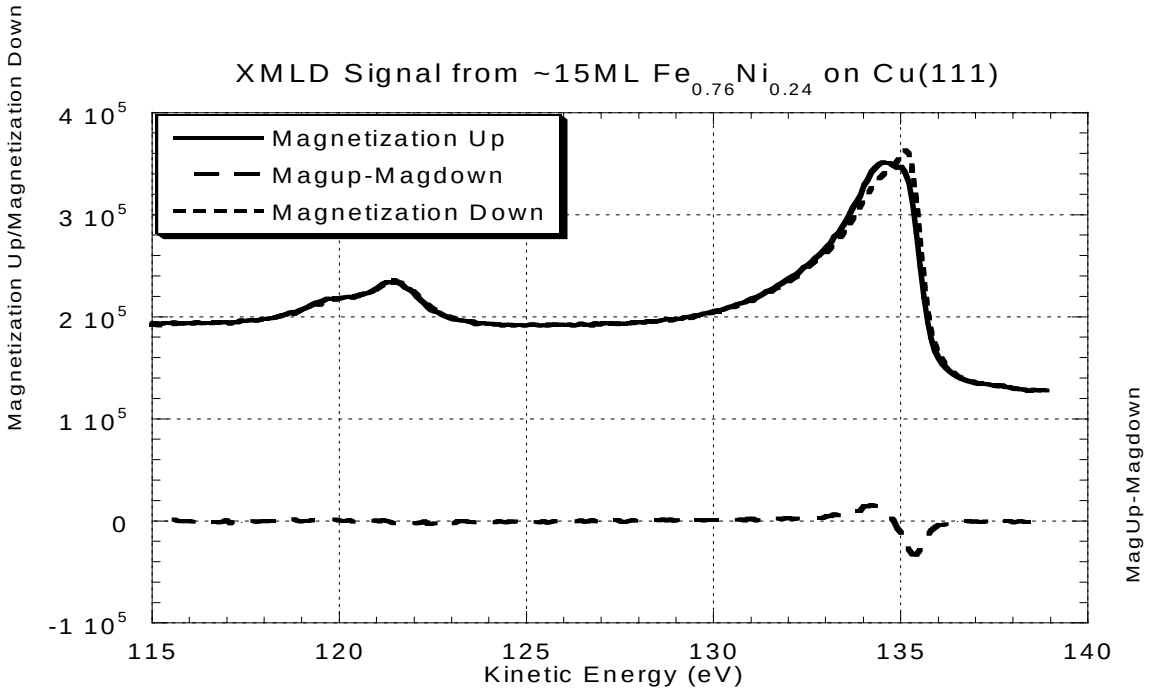

Figure 1. XMLD date from Fe-Ni thin film, 15ML thick, on Cu(111). Top of figures shows the signal for both magnetizations up and down. Bottom of figure shows difference, which is proportional to the dichroism.

Fig. 1 shows the XMLD effect for Fe concentration of 0.76 and thickness of 14ML. The upper panel clearly shows that the XPS data are different depending on the orientation of the applied field relative to the sample. The lower panel shows the difference between the two spectra in the upper panel and exhibits the dichroism effect. We have also measured the dichroism signal from both the Fe and the Ni peaks, which allows for calculation of the asymmetry.

The asymmetry is defined as, $\frac{\text{MagUp - MagDown}}{\text{MagUp + MagDown}}$, as measured from the XMLD signal.

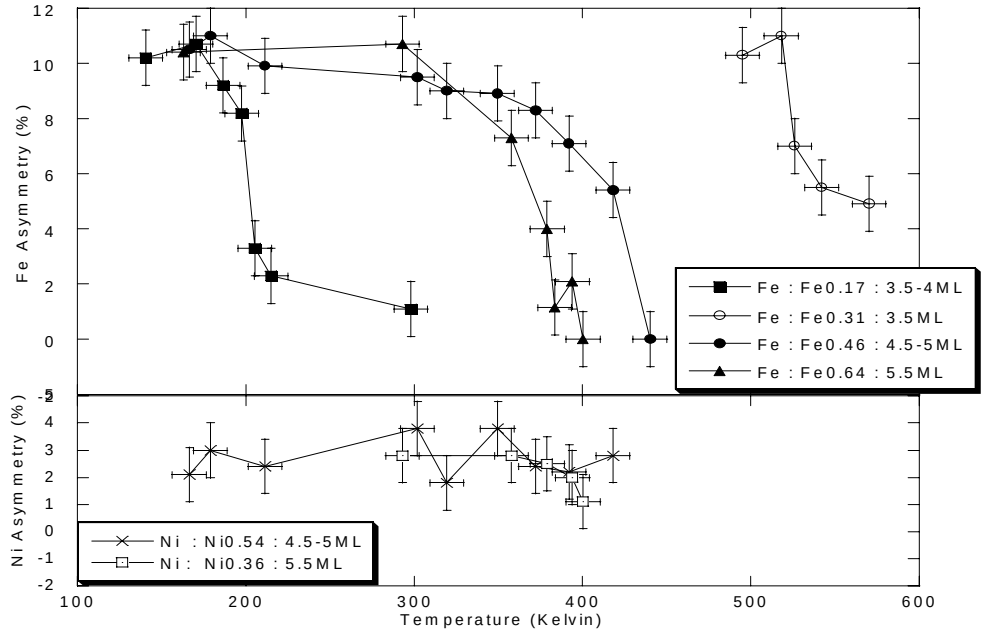

Figure 2. Fe and Ni asymmetry as a function of temperature for four Fe concentrations with film thicknesses near 5ML**.**

Figure 2 shows the asymmetry as a function of temperature for films with four different Fe concentrations and two different Ni concentrations, all ~5ML thick. The Fe data appear to fit the predictions from mean field theory, and preliminary attempts at mean field fits have had limited success. With increasing Fe concentration, the Curie temperature, where the asymmetry disappears, increases until x≈0.6, (near the Invar transition point) and then decreases.

Fig. 3 shows the total weighted asymmetry, $A_{T,}$ which is computed by performing a weighted sum of elemental asymmetries to obtain[2],

$$A_T=xA_{Fe}+(1-x)A_{Ni,},$$

with A_{Fe} and A_{Ni} being the asymmetries measured from the XMLD spectra for Fe and Ni respectively. Note that A_T also shows a magnetic instability near x=0.65. The data also support similar results by Schumann *et al* for FeNi on Cu(001). We observe that as the Fe concentration increases, we observe A_T to have an initial value of about 2%, which then monotonically increases to a maximum of about 8.5% at the Invar transition concentration. For Fe concentrations greater than x=0.65, the weighted asymmetry is quenched. As the system goes through the quenching transition, it goes from a highly aligned, high spin state to an admixture

that includes a low spin state for the Fe. For Fe on CuAu(100) multilayers, Keavney *et al*[3] also found high Fe asymmetry for Fe concentration less than or equal to 60%.

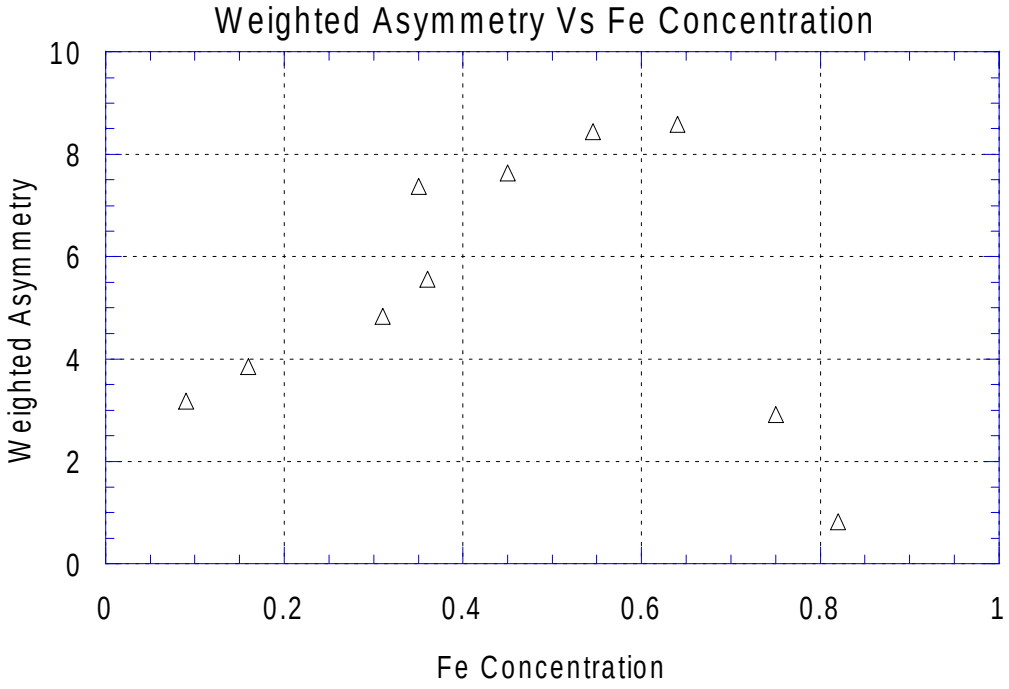

Fig. 3 Total weighted asymmetry of FeNi alloy as a function of Fe concentration for film thicknesses near 5 ML

Work is progress to compare the data in Figure 3 with previously published SQUID measurements[4] for FeNi films on Cu(111) in order to perform an absolute calibration of the XMLD signal.

REFERENCES

1. F. O. Schumann, R. F. Willis, K. G. Goodman, J. G. Tobin, Phys. Rev. Lett., **79**, 5166 (1997).
2. F. O. Schumann, R. F. Willis, J. G. Tobin, J. Vac. Sci. Tech. A **18**,1259 (2000).
3. D. J. Keavney, D. F. Storm, J. W. Freeland, I. L. Grigorov, J. C. Walker Phys. Rev. Lett., **74**, 4531 (1995).
4. J. W. Freeland, I. L. Grigorov, and J. C. Walker, Phys. Rev. B **57**, 80 (1998).

This work was supported by the Campus Laboratory Collaboration Program of the University of California Office of the President and was performed under the auspices of the U.S Department of Energy by Lawrence Livermore National Laboratory under contract no. W-7405-Eng-48. Experiments were carried out at the Spectromicroscopy Facility (Beamline 7.0) at the Advanced Light Source, built and supported by the Office of Basic Energy Sciences, U.S. Department of Energy.

Principal investigator: Shirley Chiang, Department of Physics, University of California, Davis, CA 95616-8677. Email: chiang@physics.ucdavis.edu. Telephone: 530-752-8538

X-ray spectromicroscopy of branched polyolefin blends

G. Appel[1], I. Koprinarov[2], G.E. Mitchell[2], A.P. Smith[3] and H. Ade[1]

[1]Department of Physics, North Carolina State University, Raleigh, NC 27695
[2] Analytical Sciences, The Dow Chemical Company, 1897 Building, Midland, MI, 48667
[3]National Institute of Standards and Technology, Polymers Div., Gaithersburg, MD 20899

INTRODUCTION

It is generally difficult to determine the phase diagram of polyolefin blends directly by measuring the composition of phase separated domains. The constituent materials differ only in the amount and/or length of sidechains and provide little spectroscopic differences and limited contrast in traditional miroscopies [1-3]. Indirect methods to determine the phase diagram involve a large number of samples and elaborate contrast enhancement methods. Here, we explore the utility of Near Edge X-ray Absorption Fine Structure (NEXAFS) microscopy to determine polyolefin phase diagrams directly by determining the composition of phases in a limited number of samples. We have used the scanning transmission X-ray microscope (STXM) at beamline 7.0 to investigate thermally annealed blends of an ethylene-butene copolymer (EBC with 3.7 mol % butene) and of an ethylene-octene copolymer (EOC with 3.33 mol % octene). Despite the very similar chemical structure of these copolymers (they differ only in the length of the side chain, i.e. ethyl versus hexyl groups) NEXAFS microscopy can be used to a) directly visualize the morphology without staining or etching, and b) determine the composition of the phases in such blends.

EXPERIMENTAL

0.1 % m/m solutions of EBC and EOC (experimental polymer made with single site catalyst technology) in xylene were mixed in two different ratios (samples A1-4: 33%, samples C1-4 67% EOC). Subsequently, methanol was added to precipitate the polymer. The precipitate was collected by filtering and dried. The samples were vacuum-annealed at 180°C (samples A1, C1), 160°C (samples A2, C2), 140°C (samples A3, C3) and 120°C (samples A4, C4), respectively, quenched to -7°C and cryo-microtomed to about 100-200 nm in thickness.

The data were acquired at beamline 7.0.1. C1s-NEXAFS reference spectra of the pure components were derived from line-spectra (i.e. the same line scan at many photon energies). Image sequences of up to 80 images of small areas (typically 10 μm x 10 μm) as well as small series of large images (typically 6 images, 60 μm x 60 μm) were also recorded.

RESULTS AND DISCUSSION

The C1s-NEXAFS spectra of the two components are shown in Fig. 1. The most noticeable difference between both spectra is found in the 287-288eV energy region. EBC shows two closely spaced peaks (typical for linear polyethylene or polyolefins with few or short side-chains), EOC shows only one broad signal (typical for polyolefins with many or long side-chains). These signals are interpreted as σ^*(C-H) resonances [4]. Their spectral variations primarily reflect different intermolecular distances rather than different degrees of crystallinity. These spectra were used as reference spectra during the "stack fit" procedure [5] to determine the component maps.

Fig. 2 shows typical optical density (OD) images of two of the samples. The domains of the two phases can be clearly distinguished. Because EBC shows a higher absorption coefficient at 288.2eV than EOC (see Fig. 1), regions with high EBC concentration appear bright in Fig. 2b

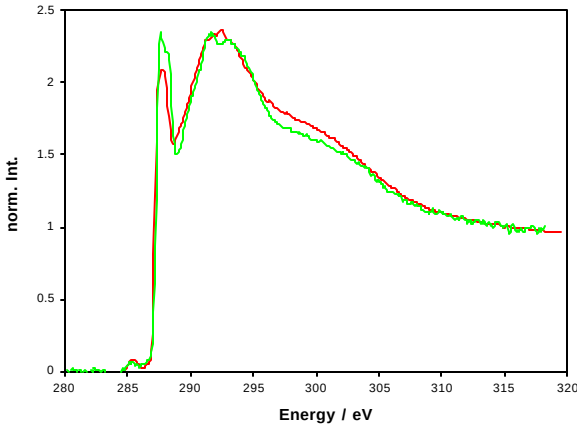

Fig. 1: C1s-NEXAFS reference spectra of the components: Red: ethylene-octene copolymer, green: ethylene-butene copolymer, both normalized to an edge jump of unity between 283eV and 315eV.

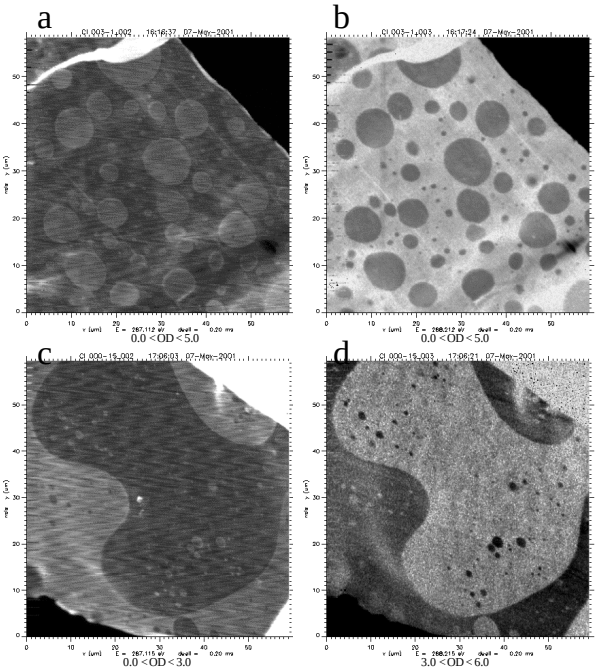

Fig. 2: Typical STXM optical density (OD) images of samples A3 (33% ethylene-octene copolymer): a), b) and C3 (67% ethylene-octene copolymer): c), d). Images a) and c) are taken at 287.1eV. Here domains, which are rich in the ethylene-octene copolymer appear bright. Images b) and d) are taken at 288.2eV and ethylene-butene rich domains appear bright in this case.

and 2d. At 287.1eV the opposite is the case and EOC rich regions appear bright. As expected from the ratio of the components in the mixed solutions, EBC forms the matrix- or majority-phase in sample A3 (a,b) and EOC in sample C3 (c,d).

After the images of an images sequence are aligned to correct for lateral shifts, the spectrum of each pixel in the stack area can be fitted by a linear combination of the reference spectra ($R_{oct}(E)$ and $R_{but}(E)$) and a constant, which is energy-independent (*constant*):

$$OD(E, x, y) = t_{oct}(x,y)*R_{oct}(E) + t_{but}(x,y)*R_{but}(E) + constant(x,y)$$

Thereby matrices of the effective thickness of the components $t_{oct}(x,y)$ and $t_{but}(x,y)$ and of the constant are determined and can be represented by component maps.

From these maps, regions in the matrix and in the minority phase were chosen carefully to not include inclusions of the other phase. Averaging over all pixels of these regions yields the effective thicknesses t. Since the sample contained only the two polymers, the composition Φ_{oct} (here the mass-fraction of EOC) can be calculated:

$$\Phi_{oct} = \frac{t_{oct}}{t_{oct} + t_{but}}$$

Thus, two composition values, one for the matrix and one for the minority phase, are derived for each sample. Fig. 3 shows these results for the different annealing temperatures. If we assume that the thermodynamical equilibrium was reached during the annealing and that the quenching conserved the composition of the melt, this diagram can be interpreted as a phase diagram. Although we presently estimate large errors (10-15%), an upper critical solution temperature behavior and a broad two-phase region is clearly visible.

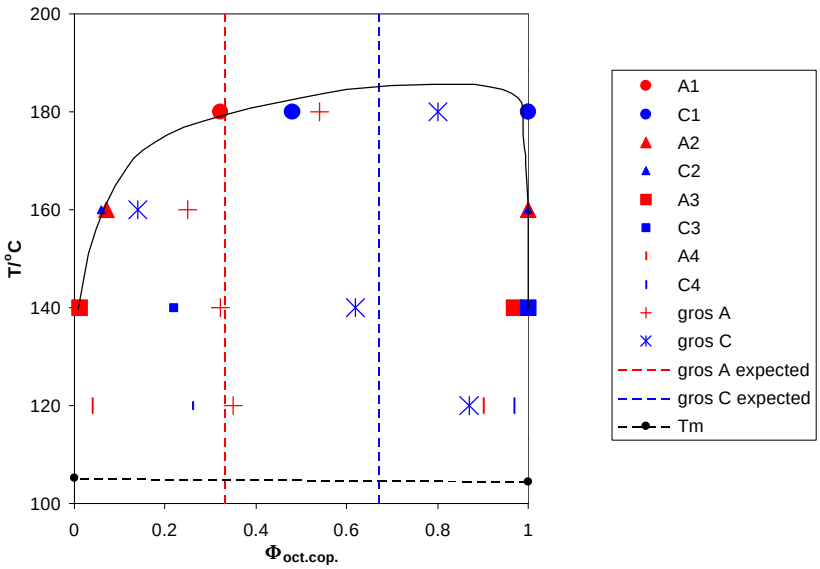

Fig. 3: Proposed phase diagram for the system poly(ethylene-ran-butene) – poly(ethylene-ran-octene). Small symbols were used, if the estimated reliability of the data was low. The gross amounts of the components from area weighted averages of the compositions and the gross amount expected from the preparation are indicated also.

In summary, we used NEXAFS-microscopy to determine the morphology and the composition of a specific polyolefin blend. The differences in the NEXAFS spectra of short- and long-branch copolymers provide sufficient image contrast, especially in the 287-288eV energy region, to image the morphology without further sample preparation (staining, etching). The polymers investigated show phase separation at all annealing temperatures. The matrix phase is always formed by the component that had the higher concentration in the solution and in the case of the EBC rich samples the gross sample composition is close to the solution composition. This indicates an almost quantitative precipitation by methanol. The phase diagram can be determined by quantitative evaluation of image sequences.

REFERENCES

1. M. J. Hill et al., Polymer **41,** 1621 (2000).
2. R. Krishnamoorti et al., J. Chem. Phys. **100,** 3894 (1994).
3. F. M. Mirabella Jr. et al., J. Polymer Sc. B 32, 2187 (1994).
4. A. Schoell A, R. Fink, E. Umbach, S. Urquhart, G.E. Mitchell, H. Ade, in preparation.
5. A. P. Hitchcock, AXIS2000 (Analysis of X-ray microscopy Images and Spectra).

This work was supported by DOE grant DE-FG02-98ER45737.

Principal investigator: Harald Ade, Department of Physics, North Carolina State University, Box 8202, Raleigh, NC 27695, e-mail: harald_ade@ncsu.edu, phone: 919 515 1331